an additional primary antibody (the third antibody) from either species. A fluorochorome-labeled secondary antibody that visualizes the third antibody is not sensitive enough to immunolabel the diluted primary antibodies that have been already visualized. Triple labeling achieved in this way, therefore, involves two antibodies from the same species, one of which should be amplified, and another antibody from different species, that can also be amplified. In this study, we used, as primary antibodies, two mouse monoclonal IgGs and a rabbit polyclonal IgG to perform triple labeling. Amplification of the signal from the rabbit polyclonal IgG and another from one of the two mouse monoclonal IgGs yielded signals intense enough to be detected in the thick sections.

2. Materials and methods

Wistar rats at postnatal day 14 (P14) were perfused transcardially with Zamboni fixative under anesthesia with inhaled diethyl ether followed by intraperitoneal administration of pentobarbital (60 mg/kg). The cerebella were taken immediately and further immersed in the same fixative overnight. After being rinsed in phosphate-buffered saline (PBS), the fixed tissues were cryoprotected by immersion in 20% sucrose in 0.1 M phosphate buffer. Floating sections with a thickness of 30 μm were obtained on a freezing microtome. Endogenous peroxidases were thoroughly inactivated by treating the sections with 2% hydrogen peroxide in PBS for 30 min. Then the sections were incubated with 5% bovine serum albumin diluted in PBS for 30 min. They were then incubated with anti-calbindin mouse monoclonal antibody of IgG class (1:2000, Swant, Bellinzona, Switzerland) at 4 °C for 3 days. In order to determine this concentration of the anti-calbindin antibody, serially diluted antibody was tested (data not shown) either with or without CARD amplification (Uchihara et al., 2003). This concentration was chosen so that the corresponding immunofluorescent signal was detectable only after CARD amplification but not without this amplification. Sections were then incubated with anti-mouse IgG made in goat conjugated with HRP (1:1000, Kirkegaard and Perry, Gaithersburg, MD). The HRP signal was intensified and visualized with tyramide conjugated with Cy5 (1:200, Perkin-Elmer, Boston, MA). Subsequent procedures were undertaken in the dark. Residual HRP was inactivated by incubating the sections in 1% hydrogen peroxide for 20 min. They were then incubated with the mixture of anti-glial fibrillary acidic protein (anti-GFAP) rabbit polyclonal antibody of IgG class (1:5000, DAKO, Glostrup, Denmark) and anti-SNAP25 mouse monoclonal antibody of IgG class (a marker for synaptic protein, SMI 81, 1:3000, Sternberger Monoclonal, Lutherville, MD) at 4 °C for another 2 days. This concentration of the anti-SNAP25 antibody was sufficient to be visualized without CARD amplification (Uchihara et al., 2003). Sections were then incubated with anti-rabbit IgG made in goat conjugated with HRP (1:500, Pierce, Rockford, IL). They were then incubated with biotinylated tyramide (1:1000, Perkin-Elmer; Adams, 1992) and the amplified signal was visualized with fluorescein-isothiocyanate (FITC) conjugated with streptavidin (1:200, Vector, Burlingame, CA). The SNAP25 epitope was visualized conventionally in parallel with an anti-mouse IgG made in sheep conjugated with rhodamine red (1:200, Jackson ImmunoRes, West Grove, PA). This anti-mouse IgG conjugated with rhodamine red visualized the anti-SNAP25 antibody at this concentration (1:3000) as determined as earlier but was not sensitive enough to visualize the anti-calbindin antibody diluted to 1:2000 (data not shown). Sections were mounted with 90% glycerol in 0.1 M phosphate buffer containing 0.1% of *p*-phenylenediamine and were observed under a confocal laser scanning microscope (Leica TCS/SP, Heidelberg, Germany). For excitation of fluorochromes, an argon–krypton laser is combined with an acoustico-optical tunable filter system, which can adjust the individual intensity of each of the three laser beams (488, 568 and 647 nm) independently. Relationship between these epitopes, probing antibodies, the corresponding fluorochromes and their excitation and emission wavelengths are shown in Table 1.

3. Results

Fig. 1 shows the triple-fluorolabeled images of the rat cerebellum at P14. Although two (calbindin: C, blue; SNAP25: B, red) of the three epitopes were probed with anti-mouse IgG of the same class, there was practically no overlap between the fluorescent signals. Each signal was captured independently and emission peak of each, measured with spectrophotometer (Leica TCS/SP), was not different from that expected from each fluorochrome used, as shown in Table 1. This confirmed that the detection

Table 1
Fluorescent dyes and their link to epitopes

Dye	Excitation wavelength (nm)	Detection range (nm)	Secondary antibody–reporter molecule	Target epitope	Color displayed
FITC–str	488	500–530	Anti-rabbit IgG–HRP[a]	GFAP	Green
Rd	568	590–630	Anti-mouse IgG–Rd	SNAP25	Red
Cy5–tyr	647	700–750	Anti-mouse IgG–HRP[a]	Calbindin	Blue

FITC: fluorescein-isothiocyanate; str: streptavidin; HRP: horseradish peroxidase; Rd: rhodamine red; tyr: tyramide.
[a] Amplified.

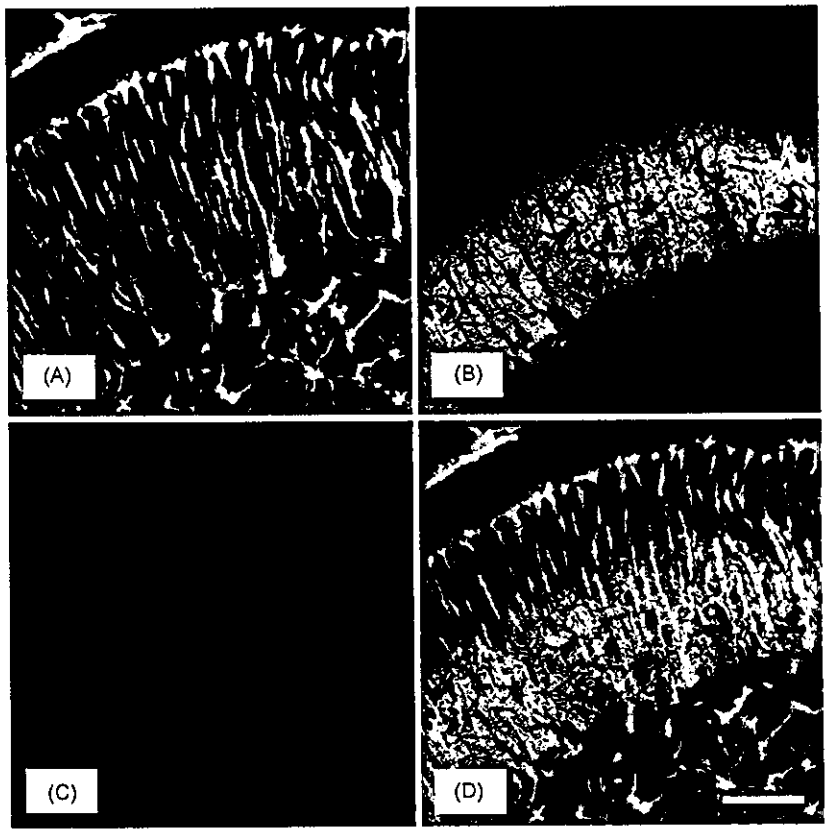

Fig. 1. Floating section (30 μm thick) from a rat cerebellum at postnatal day 14. (A) Glial fibrillary acidic protein epitope enhanced with biotinylated tyramide and visualized with streptavidin–FITC. Bergmann's glia and their processes are labeled. (B) SNAP25, a synaptic protein, probed with a mouse monoclonal antibody of IgG class without amplification through rhodamine red. (C) Calbindin probed with the other mouse monoclonal antibody of IgG class amplified and detected with tyramide–Cy5. Note the absence of cross-talk between the three immunofluorescent signals. (D) Merged image of (A)–(C) (bar = 50 μm).

system clearly distinguished each fluorochrome without cross-talk. Indeed, three different signals represented expected structures, that did not overlap with one another. Calbindin localized to Purkinje cell cytoplasm and its arborization was visualized through Cy5 (C, blue), anti-GFAP localized to Bergmann's glia and their processes was visualized through FITC (A, green) and SNAP25 in synapses accumulated in the molecular layer was visualized through rhodamine red (B, red). The merged image (D) also confirmed the absence of overlap between these signals. Omission of any of the primary antibodies was associated with disappearance of the corresponding signal (data not shown). Reversed assignment of FITC and Cy5 gave essentially the same results (data not shown). Similar triple-labeled images can be obtained at any depth of the 30 μm thick sections.

4. Discussion

We successfully performed triple immunofluorescence with two antibodies of mouse monoclonal IgG and another antibody of rabbit polyclonal IgG. Amplifying one (calbindin) of the two signals with the CARD method enabled to dilute this antibody (anti-calbindin, usually more than another 10-fold) below the threshold (Uchihara et al., 2000, 2003) that is detectable directly with the conventional secondary anti-mouse IgG conjugated with rhodamine red. This enabled to distinguish two mouse monoclonal IgGs, even though these two were probed with anti-mouse IgG. Sharp separation of signals in multiple immunolabeling is usually achieved by using primary antibodies from different species. Appropriate combination, however, is not always available, and one may be confronted with further difficulty especially when dealing with triple immunolabeling. Therefore, double labeling with two primary antibodies from the same species and class, for example, two mouse monoclonal IgGs as we demonstrated in this study, may be of great help. Direct conjugation of biotin to one of the primary antibodies may be one of the methods of choice for this purpose, but the procedure is cumbersome and requires a relatively large amount of the primary antibody (Uchihara et al., 1995). Hunyaday et al. (1996) was the first who utilized CARD amplification in this way for double fluorolabeling to obtain a good separation from non-amplified signal. Our previous study expanded this procedure by combining the third primary antibody from another species; double labeling with two rabbit polyclonal IgGs using

CARD amplification and another mouse monoclonal IgG was visualized without amplification (Uchihara et al., 2003).

Another difficulty in immunolabeling using fluorochrome-conjugated secondary antibodies is that fluorescent signals are not always sufficiently intense. CARD amplification is now often used to amplify the signal mediated by HRP targeted to the epitope. Usually, the HRP is reacted with tyramide conjugated to a reporter molecule such as biotin. Final visualization is mediated through this biotin to be linked with streptavidin-conjugated fluorochrome or HRP. In a previous study, we demonstrated that dual enhancement of double immunofluorescent signals was possible by using CARD amplification (Uchihara et al., 2000). Possible cross-reaction at the common reporter, HRP, was avoided by inactivating residual HRP with hydrogen peroxide after one of the epitopes was fluorolabeled. Subsequent cross-reaction at another common reporter, biotin, was circumvented by using fluorochromes, that are directly conjugated with tyramide. This eliminated the necessity of streptavidin for coupling between accumulated reporter (for example, biotin) and fluorochrome. Colocalization of two epitopes, ubiquitin and tau, was shown in that study (Uchihara et al., 2000), which confirmed that CARD amplification was suitable also to demonstrate colocalization of epitopes.

In the present study, employment of CARD amplification for triple immunofluorescence brought about at least two advantages; distinction between the two signals from the two mouse monoclonal IgGs and dual amplification of two fluorescent signals, one from mouse monoclonal IgG and the other from rabbit polyclonal IgG. Intensified signals enabled them to be observed throughout the entire thickness (30 μm) of the floating sections. Intensified triple immunofluorescence is now possible when just one of the three primary antibodies is from different species. This method will expand the applicability of triple immunofluorescence for research and diagnosis.

Acknowledgements

Supported in part by the grants (TU) from the Ministry of Health, Labor and Welfare (Longevity Science H-14-005) and from the Ministry of Education, Culture, Sports, Science and Technology (grant-in-aid for Scientific Research B15300118).

References

Adams JC. Biotin amplification of biotin and horseradish peroxidase signals in histochemical stains. J Histochem Cytochem 1992;40:1457–63.

Bobrow MN, Harris TD, Shaughnessy KJ, Litt GJ. Catalyzed reporter deposition, a novel method of signal amplification. Application to immunoassays. J Immunol Methods 1989;125:279–85.

Hunyaday B, Krempels K, Harta G, Mezey É. Immunohistochemical signal amplification by catalyzed reporter deposition and its amplification in double immunostaining. J Histochem Cytochem 1996;44:1353–62.

Kumar RK, Chapple CC, Hunter N. Improved double immunofluorescence for confocal laser scanning microscopy. J Histochem Cytochem 1999;47:1213–7.

Speel EJM, Ramaekers FCS, Hopman AHN. Sensitive multicolor fluorescence in situ hybridization using catalyzed reporter deposition (CARD) amplification. J Histochem Cytochem 1997;45:1439–46.

Uchihara T, Kondo H, Akiyama H, Ikeda K. Single-laser three-color immunolabeling of a histological section by laser scanning microscopy: application to senile plaque-related structures in post-mortem human brain tissue. J Histochem Cytochem 1995;43:103–6.

Uchihara T, Nakamura A, Nagaoka U, Yamazaki M, Mori O. Dual enhancement of double immunofluorescent signals by CARD: participation of ubiquitin during formation of neurofibrillary tangles. Histochem Cell Biol 2000;114:447–51.

Uchihara T, Nakamura A, Nakayama H, Arima K, Ishizuka N, Mori H, et al. Triple immunofluorolabeling with two rabbit polyclonal antibodies and a mouse monoclonal antibody allowing three-dimensional analysis of cotton wool plaques in Alzheimer disease. J Histochem Cytochem 2003;51:1201–6.

van Gijlswijk RPM, Zijlmans HJM, Wiegeant J, Bobrow MN, Erickson TJ, Adler KE, et al. Fluorochrome-labelled tyramides: use in immunocytochemistry and fluorescence in situ hybridization. J Histochem Cytochem 1997;45:375–82.

Acta Neuropathol (2004) 108 : 279–286
DOI 10.1007/s00401-004-0885-4

REGULAR PAPER

Takahiko Umahara · Toshiki Uchihara · Kuniaki Tsuchiya
Ayako Nakamura · Toshihiko Iwamoto · Kenji Ikeda
Masaru Takasaki

14-3-3 proteins and zeta isoform containing neurofibrillary tangles in patients with Alzheimer's disease

Received: 25 November 2003 / Revised: 20 April 2004 / Accepted: 28 April 2004 / Published online: 2 July 2004

Abstract Immunolocalization of 14-3-3 proteins in Alzheimer's disease (AD) brains was investigated using isoform-specific antibodies. Weak granular immunoreactivity of 14-3-3 proteins was found in neuronal cytoplasm in control subjects and AD brains. Both intracellular and extracellular neurofibrillary tangles (NFTs), as well as neuropil thread-like structures, were immunopositive for 14-3-3 proteins. This was corroborated by triple-fluorolabeling method visualizing paired helical filament (PHF) tau and 14-3-3 epitopes in relation to fibrillary state detected by thiazin red. Pretangle neurons (positive for PHF-tau without fibrillary structure detected by thiazin red) only contained fine granular immunoreactivity (IR) of 14-3-3, which was similarly found in unaffected neurons. Granular cytoplasmic IR of 14-3-3 proteins in pretangle neurons was not colocalized to granular tau-like IR, which suggests that participation of 14-3-3 proteins in NFT formation was restricted to its later stages. Its zeta isoform was most prominent in these NFTs, suggesting that this isoform is a major component involved in the formation of NFTs. In contrast, IR of epsilon isoform was found in the neuropil of the hippocampus and that of sigma isoform was localized to granule cells of the dentate gyrus in AD brains, as seen in the age-matched controls. Expression of 14-3-3 proteins were found to be highly variable and dependent on their isoforms, regions and cell types. Molecular, as well as topographical, dissection of 14-3-3 proteins will provide us with an improved understanding of this molecule in normal and pathological conditions.

Keywords 14-3-3 proteins · Zeta isoform · Alzheimer's disease · Neurofibrillary tangles · Tau protein

T. Umahara (✉) · T. Iwamoto · M. Takasaki
Department of Geriatrics, Tokyo Medical University,
6-7-1 Nishi-Shinjyuku, Shinjyuku-ku, 160-0023 Tokyo, Japan
Tel.: +81-3-33426111, Fax: +81-3-33422305,
e-mail: takahiko@tokyo-med.ac.jp

T. Umahara · T. Uchihara · A. Nakamura
Department of Neuropathology,
Tokyo Metropolitan Institute for Neuroscience,
2-6 Musashi-dai, Fuchu, 183-8526 Tokyo, Japan

K. Tsuchiya
Department of Laboratory Medicine and Pathology,
Tokyo Metropolitan Matsuzawa Hospital,
2-1-1 Kamikitazawa, Setagaya-ku, 156-0057 Tokyo, Japan

K. Ikeda
Department of Psychogeriatrics, Tokyo Institute of Psychiatry,
2-1-8 Kamikitazawa, Setagaya-ku, 156-0057 Tokyo, Japan

Introduction

14-3-3 proteins are a family of highly conserved molecule of 30 kDa [6, 9]. The proteins, first detected by Moore and Peres [23] as specific acidic proteins, are mainly localized to the synapses and neuronal cytoplasm. Although they are known as adaptor proteins, which bind to the phosphoserine-containing motifs of the target protein, they are now endowed with a growing series of potential functions and pathological relevance [5, 6, 9, 28, 30].

First, elevated 14-3-3 proteins in the cerebrospinal fluid are one of the potential indicators of transmissible spongiform encephalopathy [11], although that finding was also seen in other diseases [29]. Second, the proteins regulate intercellular signal transduction by modulating phosphorylation of the target proteins [5, 9, 12, 14, 15, 25, 31]. Third, they potentially control apoptosis induced by BAD [28, 37]. Fourth, they are colocalized to deposits, such as Lewy bodies (LBs) [17] or glial cytoplasmic inclusions (GCIs) [18, 19]: both consist of α-synuclein that shares structural homology with 14-3-3 proteins. Finally, their association to tau protein, which is the main component of neurofibrillary tangles (NFTs), first reported by Layfield et al [20] on NFTs of AD brains, was reinforced after Hashiguchi et al. [10] reported that its zeta isoform was an effector of tau phosphorylation. Recently, Agarwal-Mawal and colleagues [1] reported that the 14-3-3 zeta isoform connects glycogen synthase kinase(GSK)-3β to tau within a brain microtubule-associated tau phosphorylation complex.

Although the body of biochemical knowledge on 14-3-3 proteins is still growing and attracting increasing atten-

tion, detailed immunohistochemical studies on diseased human brains are still limited. Moreover, seven isoforms (β, γ, ε, ζ, η τ, and σ) of the protein have been so far identified in mammals [9, 21]. There were several reports concerning possible relevance of isoform specificity for disease [4, 8, 10, 21, 27, 36]. However, the physiological functions or pathological relevance of each isoform have yet to be clarified. This prompted us to investigate immunolocalization of each isoform of the 14-3-3 proteins in relation to NFTs in AD brains.

Multi-fluorolabeling with a fluorochrome, thiazin red (TR), that has an affinity to fibrillary structures such as NFTs [26, 32, 33, 34], clarified stage- and isoform-specific involvement of 14-3-3 proteins in the development of NFTs in AD brains.

Materials and methods

Hippocampal specimens were obtained from four elderly control subjects (67–85 years old) and from six patients with AD (64–83 years old, Braak's stage IV–V [7]). Five-micrometer-thick sections were obtained from formalin-fixed, paraffin-embedded blocks. After being autoclaved in a citrate buffer at 120°C for 20 min, they were treated with 1% hydrogen peroxide for 30 min. Sections were incubated with one of the primary antibodies made in rabbit (Immuno-Biological Laboratories, Gunma, Japan) against human 14-3-3 protein (1:2,000, anti-14-3-3 COM, amino acid sequence used for the epitope: KDSTLIMQLLRDNLT, without distinguishing each isoform) or its each isoform (anti-beta: MTMDKSELVQ, 1:500, anti-gamma: QQDDDGGEGNN, 1:200, anti-epsilon: EQNKEALQDVEDENQ 1:500, anti-zeta: MDKNELVQK 1:200, and anti-sigma: EEGGEAPQEPQS 1:300 isoforms) [36] at 4°C for 2 days. They were then incubated with the appropriate biotinylated secondary antibody for 2 h. After incubation with the avidin-biotin-peroxidase complex (1:1,000, ABC Elite, Vector, Burlingame, CA) for 1 h, peroxidase labeling was visualized with 0.03% 3,3-diaminobenzidine, 0.6% nickel ammonium sulfate, 0.05 M imidazole and 0.00015% hydrogen peroxide. A deep purple immunoreaction product appeared after 15–20 min.

Immunolocalization of 14-3-3 epitopes and their relation to NFTs were investigated with multi-fluorolabeling with one of the anti-14-3-3 antibodies (1:1,600 for 14-4-3 protein COM or 1:200 for anti-zeta isoform) and anti-PHF tau monoclonal antibody (1:1,000, AT8, Innogenetics, Zwijndrecht, Belgium) that recognizes phosphatase-sensitive serine199 and 202 epitopes of tau protein, but does not cross-react with normal tau proteins [22]. 14-3-3 epitopes were probed with an anti-rabbit IgG conjugated with horseradish peroxidase (1:500, Pierce, Rockford, IL) followed by amplification with biotinylated tyramide (1:1,000), and was finally visualized with streptavidin-coupled FTIC (1:200, Kirkegaard and Perry, Gaithersburg, MD). The PHF-tau epitope was simultaneously visualized with Cy5-conjugated anti-mouse IgG (1:200, Chemicon, Temecula, CA). The double-labeled sections were then immersed in 0.01 M phosphate-buffered saline containing a fluorochrome, thiazin red (TR, 1:30,000, Wako, Tokyo, Japan) that binds to fibrillary structures like NFTs [26, 32].

Sections were observed under a epifluorescence microscope combined with laser confocal system (TCS-SP, Leica, Heidelberg, Germany). FITC (emission peak: 518 nm) was detected through a 500- to 540-nm light path. TR (emission peak: 620 nm) was excited by a laser beam of 568 nm from an Ar-Kr laser and its emission was detected through 600- to 640-nm light path. Emission from Cy-5 (emission peak: 667 nm) was detected through a 660- to 730-nm light path. Each of the fluorescence signals was considered positive when it was more intense than the autofluorescence of lipofuscin granules.

After triple-stained images had been recorded, the same section was subjected to the Gallyas staining. Comparing the same field enabled the relationship between four different staining features [32, 33, 34].

Protein extraction and Western blot analyses

Extraction and Western blotting were performed as described previously [3]. Briefly, AD and control brains were homogenized and then fixed by 10% trichloroacetic acid. Each pellet was resuspended by sonication in a sample buffer containing 9 mol/l urea, 2% Triton X, and 5% 2-mercaptoethanol. Then, one fifth volume of 10% lithium dodecyl sulfate solution and approximately 2 µl of 1 mol/l TRIS solution were added to sample buffer, and the samples were sonicated again.

Lysates containing equal amounts of protein (10 µg) were subjected to 10% sodium dodecyl sulfate-polyacrylamide gel electrophoresis. Proteins were then transferred to a polyvinylidene difluoride membrane. The blots were blocked with 10%(wt/vol) skim milk and 0.1% Tween 20 in TRIS-buffered saline (TBS) at room temperature for 1 h and washed. The blots were then probed with anti-14-3-3 COM (1:2,000) or anti-14-3-3 zeta isoform (1:1,000) antibody in 1% bovine serum albumin/TBS solution at 4°C for 3 days. After three washes with 1% (wt/vol) skim milk and 0.1% Tween 20 in TBS at room temperature for 30 min, the blots were incubated with horseradish peroxidase-coupled goat anti-rabbit IgG secondary antibody (Pierce) diluted 1:4,000 with 1% (wt/vol) skim milk/TBS at room temperature for 2 h. The blots were washed three times with 0.1% Tween 20 in TBS, and visualized with the use of an enhanced chemiluminescence system (Amersham, Arlington Heights, IL).

Results

Western blot analyses

Probing human brain extracts with the anti-14-3-3 COM and zeta isoform on Western blot (Fig. 1) demonstrated a

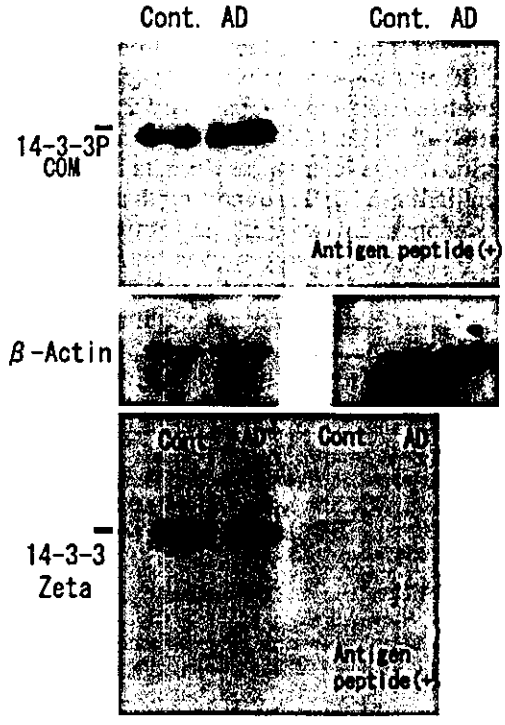

Fig. 1 Western blot of extracts from human control subject (*Cont*) and Alzheimer's disease (*AD*) brains probed with anti-14-3-3 protein (COM) and anti-zeta isoform. 14-3-3 proteins-immunoreactive bands of approximately 30 kDa are observed. *Right lanes*: spceificity control, with antibody incubated with the antigen peptide. β-Actin-immunoreactive bands are shown as control (molecular weight marker 42 kDa)

Fig. 2 14-3-3 COM IR in hippocampal sections from elderly control subjects, weak granular 14-3-3-like IR is observed in neuronal somata (*arrows*) and processes (*arrowheads*) of some hippocampal pyramidal neurons in all cases (*IR* immunoreactivity). *Bar* 100 μm

major band at approximately 30 kDa in control and AD brain. These immunopositive bands were abolished when each antigenic peptide was added to the solution containing the primary antibodies.

Fig. 3 NFTs and neuropil thread-like structures probed with anti-14-3-3 COM antibody in hippocampal sections from AD brains. A Many 14-3-3-immunoreactive NFTs. B Weak granular IR observed in neuronal somata. C Intracellular NFT, harboring a neuronal nucleus. D Extracellular NFT. E Neuropil threads-like structures intensely stained with the anti-14-3-3 COM (*NFT* neurofibrillary tangle). *Bars* A 100 μm; B–E 10 μm

Immunohistochemistry

In hippocampal sections from elderly control subjects, weak granular 14-3-3-like immunoreactivity (IR) (anti-14-3-3 COM) was observed in neuronal somata and processes of some hippocampal pyramidal neurons in all cases (Fig. 2).

In the hippocampus of AD brains, the anti-14-3-3 COM antibody immunolabeled some neurons and many NFTs (Fig. 3A). Weak granular IR was observed in some neurons (Fig. 3B). Although its intensity varied greatly, some intracellular (I-) NFTs (Fig. 3C), with tight fibrillary structure with apparently remaining nucleus [6], were strongly immunopositive for 14-3-3 proteins. IR of neuronal somata in cells that had NFTs was similar to IR of neurons that did not have NFTs. A lot of extracellular (E-) NFTs (Fig. 3D), presumably represented by thick, widely separated parallel bundles not accompanied by nucleus, were immunolabeled with this antibody, although its intensity were less intense than that of I-NFTs. In both I- and E-NFTs, this 14-3-3-like IR was not restricted to perinuclear region and extended to entire structure of NFTs. Although neuronal processes were weakly immunolabeled with the anti-14-3-3 COM antibody, strongly immunoreactive thread-like structures were observed in AD brains (Fig. 3E).

Immunohistochemical labeling was abolished when the primary antibody 14-3-3 COM and zeta isoform was coincubated with the corresponding antigen peptide (Fig. 4). We failed to demonstrate 14-3-3-like IR in senile plaques.

When probed with either anti-beta, anti-gamma or anti-zeta isoform-specific antibody against 14-3-3, NFTs in AD brains, as well as neurons in controls, exhibited immunostaining pattern similar to that observed with the anti-14-3-3 COM. Among them, labeling with anti-zeta isoform was most intense (Fig. 5A), while NFTs immunolabeled with antibodies specific for other isoforms were limited in number (data not shown).

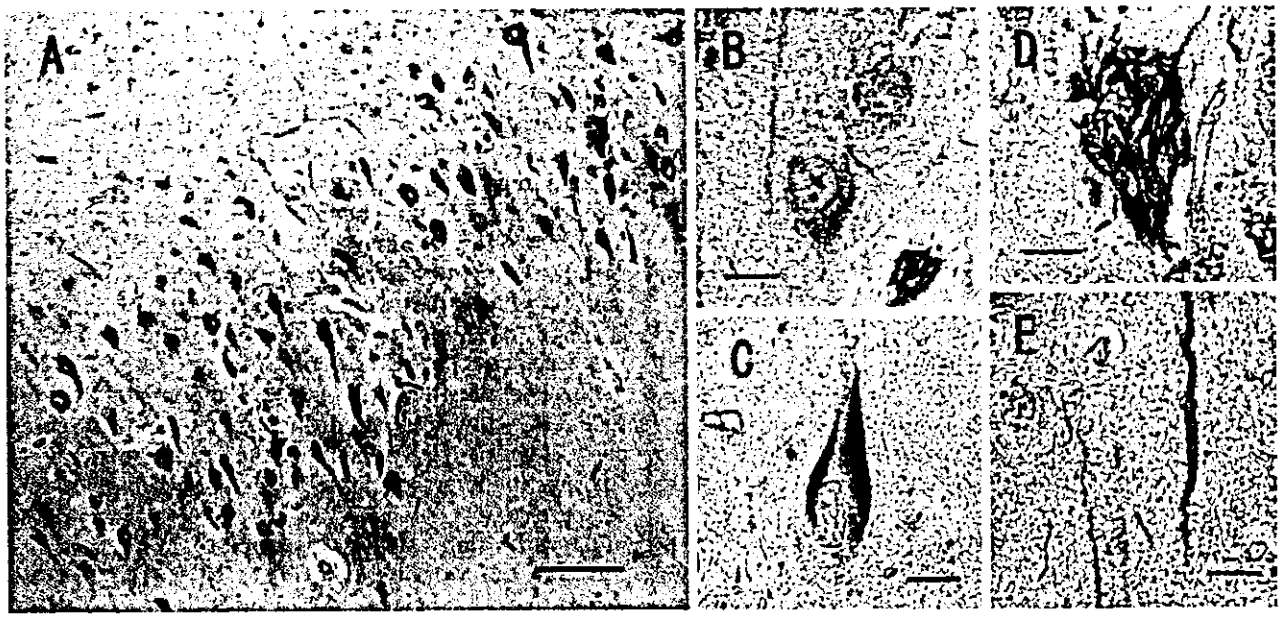

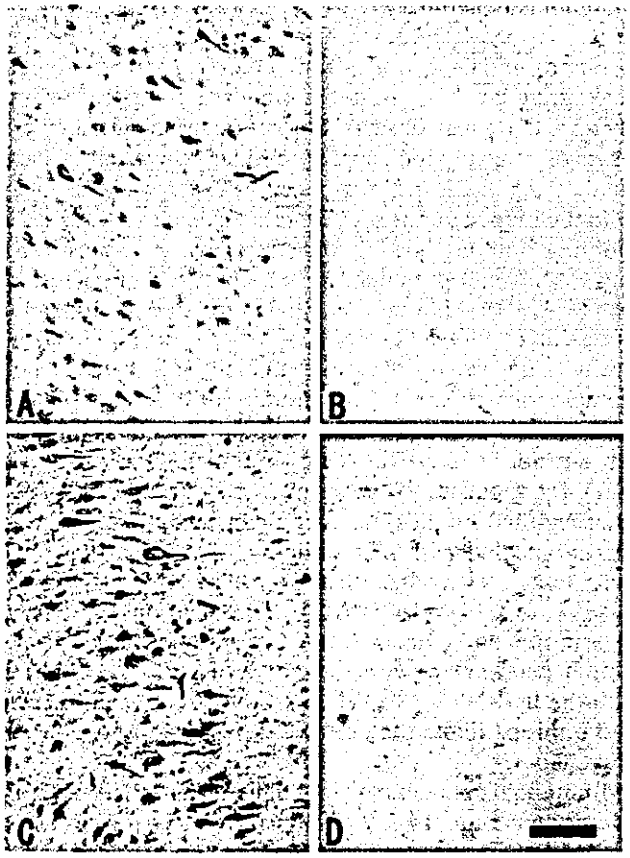

Fig. 4 **A** 14-3-3 COM-immunoreactive NFTs. **B** Immunohistochemical labeling is abolished when the primary antibody (14-3-3 COM) is coincubated with the corresponding antigen peptide. **C** Zeta isoform-immunoreactive NFTs. **D** Immunohistochemical labeling is abolished when the primary antibody (zeta isoform) is coincubated with the corresponding antigen peptide. *Bar* 100 μm

Granule cells in the dentate gyrus were intensely stained with the anti-sigma antibody both in control and AD brains (Fig. 5B). NFTs (Fig. 5B, arrow) in these granule cells were also immunostained with this antibody. Neuropil of the cerebral cortex was homogeneously stained with the anti-epsilon antibody, while neuronal soma was relatively spared (Fig. 5C). The number of NFTs labeled by this anti-epsilon antibody was limited. Some glial cells in the white matter of AD brains were also stained with this anti-epsilon antibody (Fig. 5D).

Multi-fluorolabeling study

Figure 6 shows immunolocalization of 14-3-3 COM (FITC: green) PHF-tau (AT8-Cy5: blue) and of their relation to NFTs (TR: red) in hippocampal pyramidal neurons. 14-3-3 proteins was colocalized to PHF tau and fibrillary structures of NFT (detected by thiazin red and Gallyas staining).

However, some pretangle neurons (positive for AT8 without fibrillary structure detected by thiazin red) were not immunostained with anti-14-3-3 COM antibodies (Fig. 7A). Fig. 7D shows a difference in the staining profile between a pretangle neuron, an unaffected neuron, and an NFT. This pretangle neuron only has fine granules immunolabeled with the anti-14-3-3 COM antibody, which is similarly found in unaffected neurons. Pretangle neurons have no more than few fine granules immunolabeled with this antibody.

Discussion

The present study demonstrated immunolocalization of different isoforms of 14-3-3 protein in relation to NFTs. A previous report by Layfield et al. [20] demonstrated that 14-3-3-like IR was more intense in perinuclear portion of NFTs. The present study demonstrated, in contrast, that 14-3-3-like IR was not restricted to the perinuclear portion of NFT, but was extended to the entire NFT and to neuropil threads. The antibodies used in the present study probed a single band of 30 kDa that corresponds to an expected molecular mass of 14-3-3 protein on Western blot. Immunohistochemical labeling, as well as the immunoreactive bands on Western blot, was abolished when the primary antibody was coincubated with the corresponding antigen peptide. This confirmed the specificity of the antibodies on both Western blot and immunohistochemistry. Our findings based on the antibody with documented specificity provides firm evidence that some epitopes on 14-3-3 protein are not restricted to perinuclear portion. This was further corroborated by immunolocalization of the zeta-isoform of 14-3-3 protein, again not restricted to perinuclear portion, but extended to the entire portion of NFT. Colocalization of 14-3-3 to the entire portion of NFTs was further confirmed by multi-labeling method with PHF-tau.

It has been reported that 14-3-3 protein, especially its zeta isoform, potentially binds to the microtubule-binding region of tau, regardless of phosphorylation state of tau [10]. In addition to binding of zeta isoform to tau, it potentially stimulates phosphorylation of recombinant tau by activating protein kinase A and neuronal cdc2-like kinase. Another report [1] suggests that zeta isoform dimer simultaneously binds and bridges tau and GSK3βand stimulates GSK3β-catalyzed tau phosphorylation.

One of the possibilities may be that binding of 14-3-3 protein to tau may facilitate tau phosphorylation probably at early stage of tau accumulation, that probably occurs after phosphorylation in AD brain. Our multi-labeling immunohistochemistry, however, demonstrated that it was fibrillary NFTs that were associated with 14-3-3-like IR. It failed to demonstrate 14-3-3-like IR in tau deposition not associated with fibrillary structure (so-called pretangles, as demonstrated by tau-like IR without TR staining) [32, 33, 34]. If these non-fibrillar tau-deposits represent early stage of NFT formation, the immunohistochemical findings in the present study is not compatible with possible participation of 14-3-3 in tau phosphorylation at least in the early stage of NFT formation. Association of 14-3-3 proteins to fibrillar tau deposits as NFT may suggest potential roles of this protein either in later stage of NFT for-

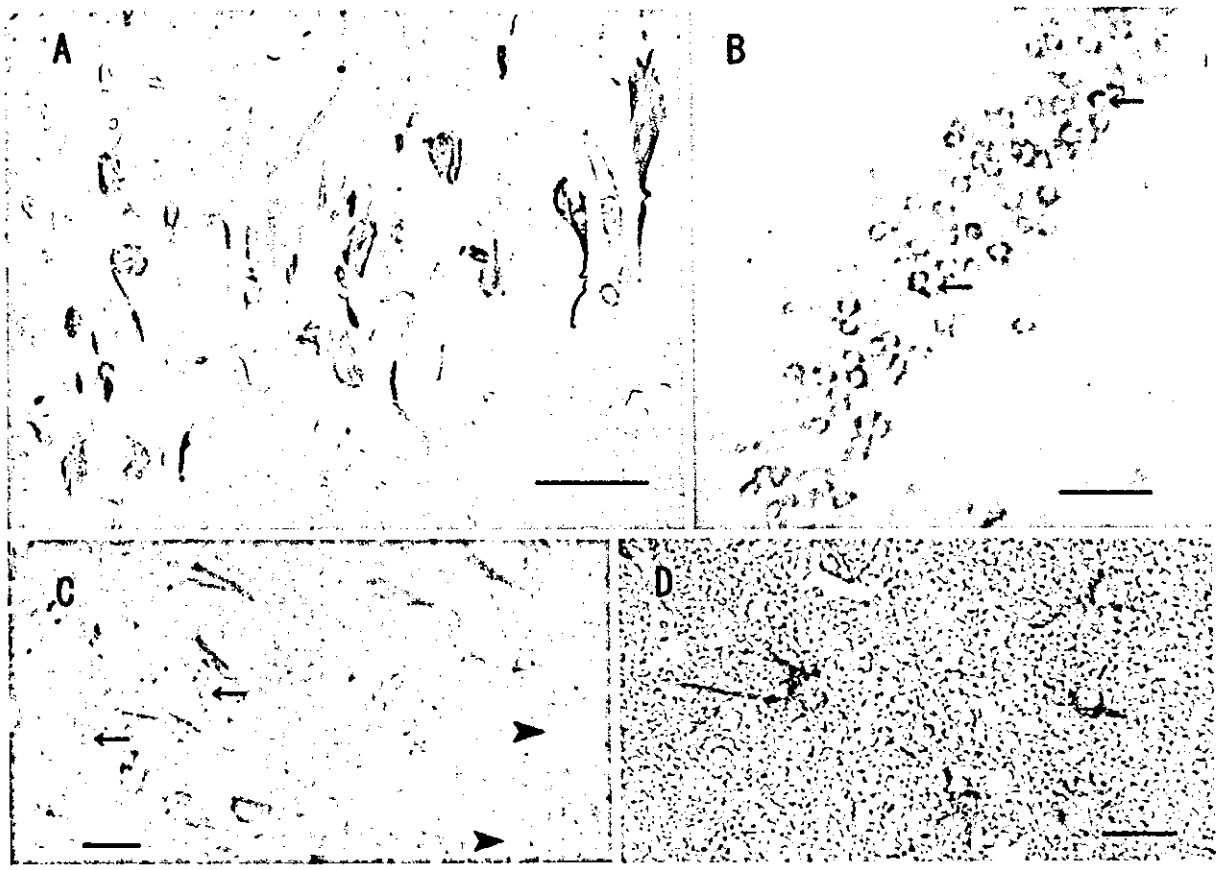

Fig. 5 Immunolocalization of zeta, sigma and epsilon isoforms of 14-3-3 proteins. **A** Zeta isoform-containing NFTs in hippocampal sections from AD brains. **B** Granule cells in the dentate gyrus are stained with the anti-sigma isoform antibody in AD brain. NFTs in granular cells in the dentate gyrus are strongly stained (*arrows*). **C** Neuropil of the hippocampus are homogeneously stained with the anti-epsilon isoform antibody, while neurons (*arrows*) and process (*arrowheads*) are relatively spared. **D** Some glial cells in the white matter of AD brains are also positive for the epsilon isoform. **A, B, D** 50 μm; **C** 20 μm

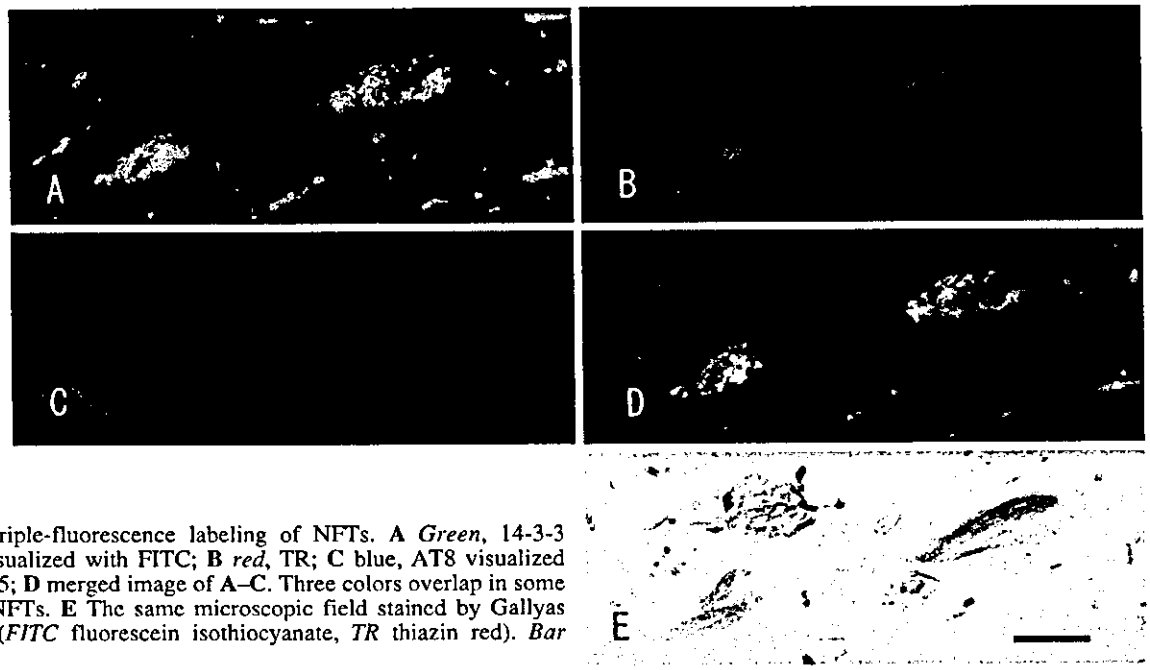

Fig. 6 Triple-fluorescence labeling of NFTs. **A** *Green*, 14-3-3 COM visualized with FITC; **B** *red*, TR; **C** blue, AT8 visualized with Cy-5; **D** merged image of **A–C**. Three colors overlap in some part of NFTs. **E** The same microscopic field stained by Gallyas method (*FITC* fluorescein isothiocyanate, *TR* thiazin red). *Bar* 25 μm

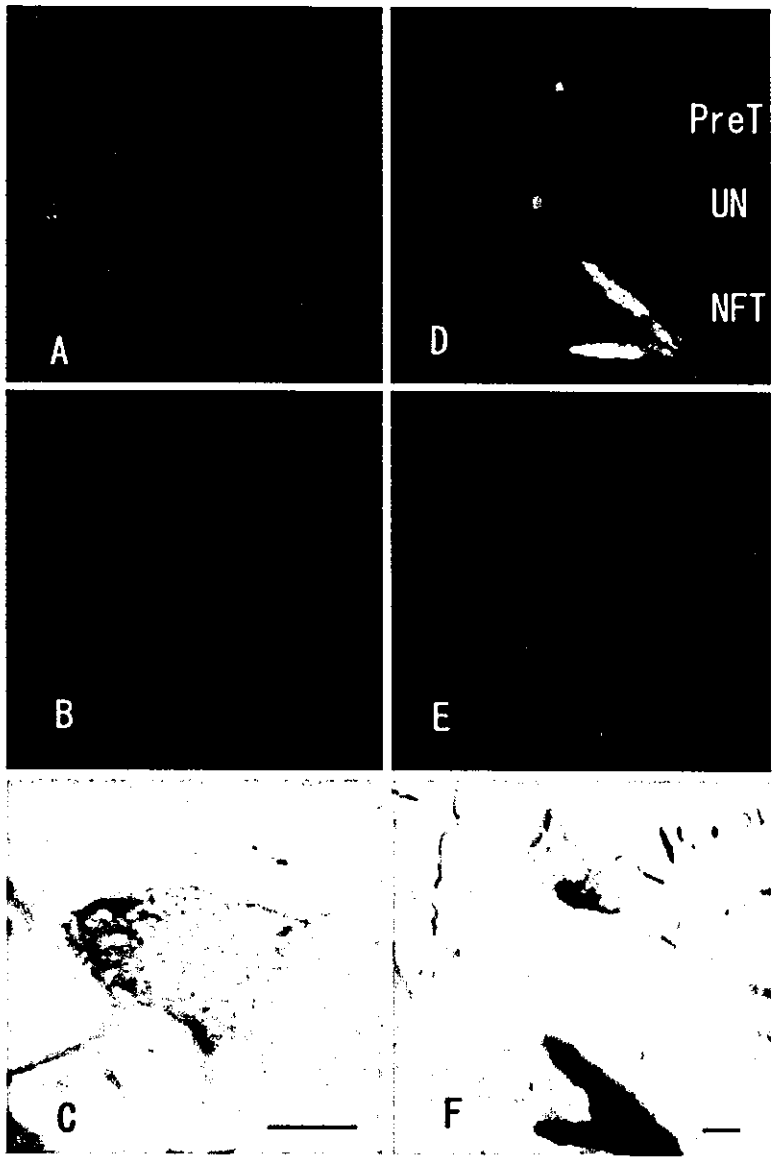

Fig. 7 A Triple-fluorescence labeling of a pretangle neuron. Merged image of 14-3-3 COM (*green*), TR (*red*) and AT8 (*blue*). B IR of 14-3-3 COM (*green*). C The same microscopic field stained by Gallyas method. IR of 14-3-3 proteins is not seen in this structure. D shows a pretangle neuron (*PreT*), an unaffected neuron (*UN*), and an NFT (merged image). This pretangle neuron only has fine granules immunolabeled by anti-14-3-3 COM antibody, which is similarly found in unaffected neuron. E IR of 14-3-3 COM (*green*). F The same microscopic field stained by Gallyas method. *Bars* 10 μm

Table 1 Immunoreactivity of hippocampus section by anti-14–3-3 proteins (*AD* Alzheimer's disease, *Control* elderly control subject, *NFTs* neurofibrillary tangles, *I-* intracellular, *E-* extracellular, *N-Th* neuropil threads)

Antibodies	AD			Control
	NFTs	N-Th	Others	
14–3-3 (common)	+++ I-NFTs, E-NFTs	+	Neuronal somata and processes	Neuronal somata and processes
Zeta	+++	+	Neuronal somata and processes	Neuronal somata and processes
Beta, gamma	+	±	Neuronal somata and processes	Neuronal somata and processes
Sigma	+	±	Granule cells in dentate gyrus	Granule cells in dentate gyrus
Epsilon	+	±	Neuropil and glial cells	Neuropil

mation or in functions related to neither tau deposition nor NFT formation. Indeed, NFT is not the only structure that contains 14-3-3 epitopes. For example, recent studies reported that GCIs in multiple system atrophy [18, 19] or Lewy bodies [17] are also rich in 14-3-3 epitopes. We do not yet know whether these cytoplasmic inclusions, more or less fibrillar in nature, share a common pathological cascade that involves 14-3-3 protein. Apart from these fibrillary inclusions, 14-3-3-like IR was also noted in the cytoplasm of neurons even in the presence of NFT. Because the presence of NFT did not influence the apparent intensity of this cytoplasmic 14-3-3-like IR, 14-3-3 protein may also be involved in processes not directly related to formation of fibril or inclusions.

In the present study, we used a panel of antibodies specific for each isoforms of 14-3-3 proteins (Table 1), since

there are few immunohistochemical studies using isoform-specific antibody in human brains. In control brains, beta, gamma, and zeta isoform-specific antibody showed findings almost similar to those obtained with the 14-3-3 COM antibody. Among them, it was the zeta isoform that immunolabeled many NFTs. This suggests that the zeta isoform is the major isoform deposited in NFT with fibrillary structure.

In contrast, immunolabeling of granule cells in the hippocampal dentate gyrus with the anti-sigma isoform antibody was enhanced in AD brains. This group of neurons are now attracting particular attention for their potential of neurogenesis [2, 16]. Moreover, peculiar tau-immunoreactive inclusions [24] were frequently found in these neurons in Pick body disease [35] or frontotemporal dementia linked to chromosome 17 [13]. Behaviors of these neurons may be distinct from what we observed on pyramidal neurons in hippocampus or cerebral cortex. If 14-3-3 proteins are involved in degenerative or regenerative processes, difference in expression of 14-3-3 protein isoforms may be linked to regional difference in these processes. This hypothesis, however, awaits confirmation.

Baxter et al. [4] reported that IR of the epsilon isoform was found in the gray matter of murine brain. Our results on human brain tissue were in agreement with theirs and are compatible with the hypothesis that epsilon isoform is closely associated synapses [4].

Although association of 14-3-3 epitopes has been described in a variety of fibrillary structures and inclusions [10, 17, 18, 19], there are some fibrillary deposits, for example senile plaques of AD, that apparently lack 14-3-3-like IR, as we confirmed in this study [27]. These indicate that fibrillary structures are not necessarily associated with 14-3-3-like IR. Moreover, it is interesting that some prion protein (PrP) deposits in Creutzfeldt-Jakob disease exhibit 14-3-3-like IR, while those in Gerstmann-Sträussler-Scheinker syndrome lack 14-3-3-like IR [27]. This contrast implies that conformational difference of the PrP, possibly explaining different morphologies of PrP plaques, is related to deposition of 14-3-3 protein. However, it remains to be clarified whether deposition of 14-3-3 is a secondary event dependent on preformed conformation or whether the deposition of 14-3-3 protein alters the conformation of other molecules to form deposits or inclusions.

The present study demonstrated that expression of 14-3-3 protein was highly variable and dependent on their isoforms, regions and cell types. Because each isoform has different functions under different conditions [4, 8, 10, 21, 27, 36], quantitative changes of 14-3-3 proteins in AD brains reported by Fountoulakis et al. [8] would be duly interpreted if data on cellular localization and regional difference are provided. Molecular, as well as topographical, dissection of 14-3-3 protein and its isoforms in relation to normal and pathological functions and structures will provide us with improved understanding of this molecule.

Acknowledgement This work is supported in part by grants for Sumitimo Welfare Foundation.

References

1. Agarwal-Mawal A, Qureshi HY, Cafferty PW, Yuan Z, Han D, Lin R, Paudel HK (2003) 14-3-3 connects glycogen synthase kinase-3β to tau within a brain microtubule-associated tau phosphorylation complex. J Biol Chem 278:12722–12728
2. Alyoman J, Das GD (1965) Autoradiographic and histological evidence of postnatal hippocampal neurogenesis in rats. J Comp Neurol 124:319–336
3. Aoki K, Uchihara T, Sanjo N, Nakamura A, Ikeda K, Tsuchiya K, Wakayama Y (2003) Increased expression of neuronal apolipoprrptein E in human brain with cerebral infarction. Stroke 34:875–880
4. Baxter HC, Liu WG, Forster JL (2002) Immunolocalisation of 14-3-3 isoforms in normal and scrapie-infected murine brain. Neuroscience 109:5–14
5. Berg D, Holzmann C, Riess O (2003) 14-3-3 proteins in the nervous system. Nat Rev Neurosci 4:752–762
6. Boston PF, Jackspn P, Thompson RJ (1982) Human 14-3-3 protein: radioimmunoassay, tissue distribution, and cerebrospinal fluid levels in patients with neurological disorders. J Neurochem 38:1475–1482
7. Braak H, Braak A (1991) Neuropathological stageing of Alzfeimer-related changes. Acta Neuropathol 82:239–259
8. Fountoulakis M, Cairns N, Lubec G (1999) Increased levels of 14-3-3 gamma and epsilon proteins in brain of patients with Alzheimer's disease and Down syndrome. J Neural Transm 57: 323–335
9. Fu H, Subramanian RR, Masters SC (2000) 14-3-3 protains: structur, function, and regulation. Annu Rev Pharmacol Toxicol 40:617–647
10. Hashiguchi M, Sobue K, Paude HP (2000) 14-3-3 ζ is an effector of tau protein phosphorylation. J Biol Chem. 275: 25247–25254
11. Hsich G, Kenney K, Gibbs CJ, Lee KH, Harrington MG (1996) The 14-3-3 protain in cerebrospinal fluid as a maker for transmissible spongiform encephalopathy. N Engl J Med 335:924–930
12. Ichihara T, Isobe T, Okuyama T, Yamauchi T, Fujisawa H (1987) Brain 14-3-3 protein is an activator protein that activates tryptophan 5-monooxygenase and tyrosine 3-monooxygenase in the presence of Ca^{2+}, calmodulin-dependent protein kinase II. FEBS Lett 219:79–82
13. Iizima M, Tabira T, Poorkaj P, Schellenberg GD, Trojanowski JQ, Lee VM, Schmidt ML, Takahiashi K, Nabika T, Matsumoto T, Yamashita Y, Yoshioka S, Ishino H (1999) A distinct familial presenil dementia with a novel missense mutation in the tau gene. Neuroreport 25:497–501
14. Jones DH, Ley S, Aiken A (1995) Isoforms of 14-3-3 protein can form homo- and heterodimers in vitro: implications for function as adaptor proteins. FEBS Lett 368:55–58
15. Jones DH, Martin H, Madrazo J, Robinson KA, Nielson P, Roseboom PH, Patel Y, Howell SA, Aitken A (1995) Expression and structural analysis of 14-3-3 proteins. J Mol Biol 245:375–384
16. Kaplan MS, Bell DH (1984) Mitotic neuroblasts in the 9-day-old and 11-month-old rodent hippocampus. J Neurosci 4:1429–1441
17. Kawamoto Y, Akiguchi I, Nakamura S, Honjyo Y, Shibasaki H, Budka H (2002) 14-3-3 proteins in Lewy bodies in Parkinson disease and diffuse Lewy body disease brain. J Neuropathol Exp Neurol 61:245–253
18. Kawamoto Y, Akiguchi I, Nakamura S, Budka H (2002) Accumulation of 14-3-3 proteins in glial cytoplasmic inclusions in multiple system atrophy. Ann Neueol 52:722–731
19. Komori T Ishizawa K Arai N Hirose T Mizutani T Oda M (2003) Immunoexpression of 14-3-3 proteins in glial cytoplasmic inclusions of multiple system atrophy. Acta Neuropathol 103:66–70

20. Layfield R, Fergusson J, Aitken A, Lowe J, Landon L (1996) Neurofibrillary tangles of Alzheimer's desease brain contain 14-3-3 protain. Neurosci Lett 209:57–60
21. Martin H, Rostas J, Patel Y, Aitken A (1994)Subcellular localisation of 14-3-3 isoforms in rat brain using specific antibodies. J Neurochem 63:2259–2265
22. Mercken M, Vandermeeren M, Lubke U, Six J, Boons J, Van de Voorde A, Martin J-J, Gheuens J (1992) Monoclonal antibodies with selective specificity for Alzheimer tau are direcred against phosphatase-sensitive epitope. Acta Neuropathol 84: 265–272
23. Moore BW, Perez VJ (1967) In: Carlson FD (ed) Physiological and biochemical aspects of nervous integration. Prentice-Hall, New Jersey, pp 343–359
24. Murayama S, Nukina N, Ihara Y, Nakazato Y, Ishida Y, Takanashi R (1985) Immunocytochemistry of Pick's argentophilic bodies: evidence for the involvement of high molecular weight microtubule-associated proteins (HMWP) before the appearance of tubulin (in Japanese). Rinsho Shinkeigaku 25: 80–87
25. Muslin AJ, Tanner JW, Allen PM, Shaw AS (1996) Interaction of 14-3-3 with signaling proteins is mediated by the recognition of phosphoserine. Cell 84:889–897
26. Resch JF, Lehr GS, Wischik CM (1991) Design and synthesis of a potential affinity cleaving reagent for beta-pleated sheet protein structures. Bioorg Med Chem Lett 1:519–522
27. Richard M, Biacabe A-G, Streichnberger N, Ironside JW, Mohr M, Kopp Nicolas, Perret-Liauded A (2003) Immunohistochemical localization of 14-3-3ζprotein in amyloid plaques in human spongiform encephalopathies. Acta Neuropathol 105:296–302
28. Rosenquist M (2003) 14-3-3 proteins in apoptpsis. Braz J Med Biol Res 36:403–408
29. Satoh J, Kurohara K, Yukitake M, Kroda Y (1999) The 14-3-3 protain detectable in the cerebraospinal fluid of patients with prion-unrelated neurological diseases is expressed constitutively in neuronal and glial cells in culture. Eur Neurol 41: 216–225
30. Skoulakis EMC, Davis RL (1998) 14-3-3 protains in neuronal development and function. Mol Neurobiol 16:269–284
31. Tzivion G, Avruch J (2001) 14-3-3 proteins: active cofactors in cellular regulation by serine/threonine phosphorylation. J Biol Chem 14:3061–3064
32. Uchihara T, Nakamura A, Yamazaki M, Mori O (2000) Tau-positive neurons in corticobasal degeneration and Alzheimer disease-distinction by thiazin red and silver impregnations. Acta Neuropathol 100:385–389
33. Uchihara T, Nakamura A, Yamazaki M, Mori O (2001) Evolution from pretangle neurons to neurofibrillary tangles monitored by thiazin red combined with Gallyas method and double immunofluorescence. Acta Neuropathol 101:535–539
34. Uchihara T, Nakamura A, Yamazaki M, Mori O, Ikeda K, Tsuchiya K (2001) Different conformation of neuronal tau deposits distinguished by double immunofluorescence with AT8 and thiazin red and combined with Gallyas method. Acta Neuropathol 102:462–466
35. Uchihara T, Ikeda K, Tsuchiya K (2003) Pick body disease and Pick syndrome. Neuropathology 23:318-326
36. Wakabayashi H, Yano M, Tachikawa N, Oka S, Maeda M, Kido H (2001) Increased concentration of 14-3-3 epsilon, gamma, and zeta isofrms in cerebrospinal fluid of AIDS patients with neuronal destruction. Clin Chim Acta 312:97–105
37. Zha J, Harada H, Yang E, Jockel J, Korsmeyer SJ (1996) Serine phosphorylation of death agonist BAD in response to survival factor results in binding to 14-3-3 not BCL-X(L). Cell 87:619–692

Available online at www.sciencedirect.com
SCIENCE DIRECT
Neuroscience Letters 371 (2004) 215–219
Neuroscience Letters
www.elsevier.com/locate/neulet

Immunolocalization of 14-3-3 isoforms in brains with Pick body disease

Takahiko Umahara[a,b,*], Toshiki Uchihara[b], Kuniaki Tsuchiya[c], Ayako Nakamura[b], Kenji Ikeda[d], Toshihiko Iwamoto[a], Masaru Takasaki[a]

[a] Department of Geriatrics, Tokyo Medical University, 6-7-1 Nishi-Shinjyuku, Shinjyuku-ku, Tokyo 160-0023, Japan
[b] Department of Neuropathology, Tokyo Metropolitan Institute for Neuroscience, 2-6 Musashi-dai, Fuchu, Tokyo 183-8526, Japan
[c] Department of Laboratory Medicine and Pathology, Tokyo Metropolitan Matsuzawa Hospital, 2-1-1 Kamikitazawa, Setagaya-ku, Tokyo 156-0057, Japan
[d] Department of Psychogeriatrics, Tokyo Institute of Psychiatry, 2-1-8 Kamikitazawa, Setagaya-ku, Tokyo 156-0057, Japan

Received 15 December 2003; received in revised form 23 August 2004; accepted 30 August 2004

Abstract

Immunolocalization of 14-3-3 protein isoforms in relation to Pick bodies in Pick body disease (PBD) brains was investigated. Weakly granular immunoreactivity of 14-3-3 proteins was found in neurons in control subjects and in Pick body disease brains. In addition to this granular immunoreactivity, many Pick bodies were immunopositive for 14-3-3 proteins as confirmed with double-immunofluorescence with an anti-PHF tau (AT8) and anti-14-3-3 that recognizes all its isoforms (common). When probed with isoform-specific antibodies, Pick bodies were positive for beta, gamma, epsilon, eta, tau, and zeta isoform and exhibited immunostaining pattern similar to that observed with the anti-14-3-3 proteins (common). In addition, immunoreactivity of sigma isoform, so far considered to be exclusively extraneuronal, was unexpectedly found in Pick bodies, normal hippocampal neurons and brain homogenate from age-matched controls. Although localization of 14-3-3 proteins in Pick bodies suggests their involvement in Pick body formation, their role may be variable dependent on the isoforms differently expressed in different area in the brain.

Keywords: 14-3-3 proteins; Sigma isoform; Pick body; Pick body disease; Tau protein; Granule cells of the dentate gyrus

14-3-3 proteins are a family of highly conserved molecule of 30 kDa [5]. The proteins are mainly localized to the synapses and neuronal cytoplasm. Although they are known as adaptor proteins, which bind to the phosphoserine-containing motifs of the target protein, they are now endowed with a growing series of potential functions and pathological relevance [3,5,8,13].

Elevated 14-3-3 proteins in the cerebrospinal fluid are one of the potential indicators of transmissible spongiform encephalopathy [7]. The proteins regulate intercellular signal transduction by modulating phosphorylatin of the target proteins [3,5,8], and control apoptosis induced by BAD [13,18]. They are colocalized to a variety of deposits characteristic for some neurodegenerative processes, such as Lewy bodies (LBs) [10] or glial cytoplasmic inclusions (GCIs) [9,11] both consist of α-synuclein that shares structural homology with 14-3-3 proteins, and neurofibrillary tangles (NFTs) in Alzheimer's disease (AD) brains [12,16]. This raises the possibility that 14-3-3 proteins play some indispensable roles during formation of these deposits regardless of the diagnosis and prompted us to examine Pick bodies, another example of a disease-specific deposits. Seven isoforms (β: beta; γ: gamma; ε: epsilon; ζ: zeta; η: eta; τ: tau; and σ: sigma) of the protein have been so far identified in mammals [5]. However, physiological functions or pathological relevance of each isoform are yet to be clarified. We then decided to undertake an immunohistochemical study on a series of brains with Pick body disease (PBD) [15] or Pick's disease with Pick bodies [14] with

* Corresponding author. Tel.: +81 3 3342 6111; fax: +81 3 3342 2305.
E-mail address: takahiko@tokyo-med.ac.jp (T. Umahara).

0304-3940/$ – see front matter © 2004 Elsevier Ireland Ltd. All rights reserved.
doi:10.1016/j.neulet.2004.08.079

a panel of antibodies specific for each isoform known to date.

In this study, we used following primary antibodies (Immuno-Biological Laboratories, Gunma, Japan), raised in rabbit against human 14-3-3 protein (1:2000, anti-14-3-3 COM raised against common sequence KDSTLIMQLLRDNLT shared by all isoforms) or its each isoform (anti-beta MTMDKSELVQ: 1:500, anti-gamma QQDDDGGEGNN: 1:200, anti-epsilon EQNKEALQDVEDENG: 1:500, anti-zeta MDKNELVQK: 1:200, and anti-sigma (C) EEGGEAPQEPQS: 1:300, anti-eta MGDREQLLQR, isforms) and used anti-14-3-3 tau isoform monoclonal antibody (raised against recombinant human 14-3-3 tau) [17]. Specificity of six of these antibodies (14-3-3 COM, beta, gamma, epsilon, zeta, and sigma isoforms) was established previously on Western blot [16,17] and absorption studies (14-3-3 COM and zeta isoform) [16]. Other antibodies were tested for their specificity for each isoform on Western blot (sigma isoform) and by absorption of immunolabeling upon coincubation with the antigen peptide, as described below. Briefly, control brains [2] were homogenized in an ice-cooled fixative 10% trichloroacetic acid. Each pellet was solubulized by sonication in a sample buffer containing 9 mol/L urea, 2% Triton X, and 5% 2-mercaptoethanol. Then one-fifth volume of 10% lithium dodecyl sulfate solution and approximately 2 μL of 1 mol/L Tris solution were added to sample buffer, and the samples were sonicated again.

Lysates containing equal amounts of protein (20 μg) were subjected to 10% sodium dodecyl sulfate-poly-acrylamide gel electrophoresis. Transferred protein were probed with the anti 14-3-3 sigma isoform (1:200) antibody and visualized with the use of an enhanced chemiluminescence system (Amersham, Arlington Heights, IL).

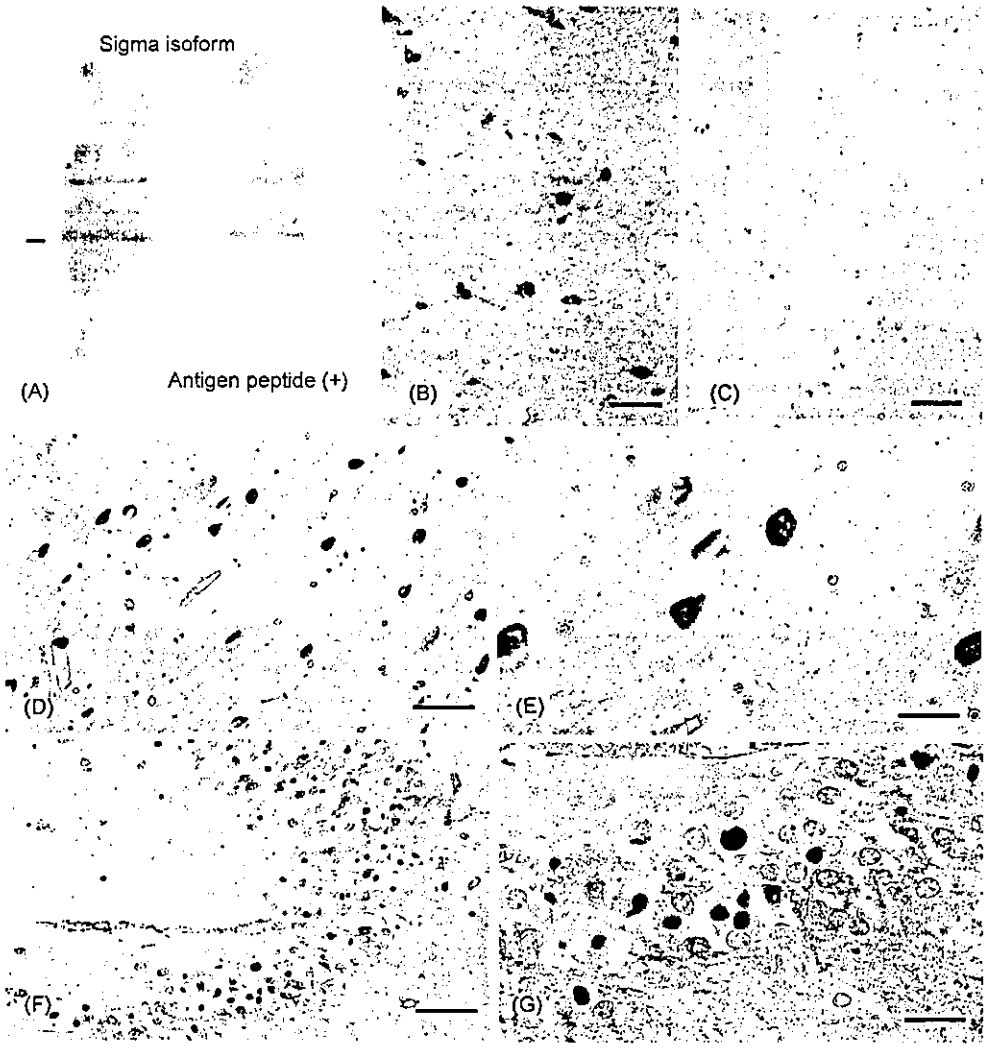

Fig. 1. Pick bodies probed with anti-14-3-3 antibodies in hippocampal sections from Pick body disease brains. (A) Western blot of extracts from human control subject brains probed with the anti-sigma isoform antibody. A faint band at approximately 30 kDa is detectable (left panel), which is abolished when coincubated with the antigen peptide (right panel). Bar: 30 kDa. (B) 14-3-3 common (COM)-immunoreactive Pick bodies. (C) This immunoreactivity was abolished when the antigen peptide was added to the solution containing the primary antibody. (D–G) Pick bodies in hippocampal pyramidal neurons (D and F) and in granule cells in the dentate gyrus (F and G) were clearly immunolabeled by 14-3-3 COM. Bar (B–D and F) 50 μm; (E and G) 20 μm.

In our previous report, probing human brain extracts with the anti-14-3-3 COM and zeta isoform demonstrated a major band at approximately 30 kDa in control and AD brain [16]. In this study, that of the anti-sigma isoform similarly demonstrated a faint band at approximately 30 kDa in the brain homogenate. This immunopositive band was abolished when the antigenic peptide was added to the solution containing the primary antibody (Fig. 1A).

With these isoform-specific antibodies, immunolocalization of each epitope was examined on hippocampal specimens obtained from four elderly control subjects (67–85 years old) and from four patients with PBD (56–83 years old). Five micronmeter-thick sections were obtained from formalin-fixed, paraffin-embedded blocks. After being autoclaved in a citrate buffer at 120 °C for 20 min, they were treated with 1% hydrogen peroxide for 30 min. Sections were incubated with one of the primary antibodies for 2 days.

They were then incubated with the appropriate biotinylated secondary antibody for 2 h at a dilution of 1:1000. After incubation with the avidin–biotin-peroxidase complex (1:1000, ABC Elite, Vector Laboratories, Burlingame, CA) for 1 h, peroxidase labeling was visualized with 0.03% 3,3-diaminobenzidine, 0.6% nickel ammonium sulfate, 0.05 M imidazole and 0.00015% hydrogen peroxide. A deep purple immunoreaction product appeared after 15–20 min.

Immunolocalization of 14-3-3 epitopes and their relation to Pick body were further investigated with double-fluorolabeling with the anti 14-3-3 COM antibody (1:1600) and an anti-PHF tau monoclonal antibody (1:1000, AT8, Innogenetics, Zwijndrecht, Belgium) that recognizes phosphatase-senseitive serine 199 and 202 epitopes of tau protein but does not cross-react with normal tau proteins. 14-3-3 epitopes were probed with an anti-rabbit IgG conjugated with horseradish peroxidase (1:500, Pierce, Rockford, IL) followed by amplification with biotinylated tyarmide (1:1000), and was finally visualized with streptavidin-coupled FTIC (1:200, Vector Laboratories, Burlingame, CA). The PHF-tau epitope was simultaneously visualized with anti-mouse IgG (Fc γ-fragment specific) coupled with Rhodamin Red (1:200, Jackson ImmunoReseach, West Grove, PA).

Sections were observed under an epifluorescence microscope combined with laser confocal system (TCS-SP, Leica, Heidelberg, Germany). FITC (emission peak: 518 nm) was detected through a 500–540 nm light path. Emission from Rhodamin Red (emission peak: 590 nm) was detected through a 590–620 nm light path. Each of the fluorescence signals was considered positive when it was more intense than the autofluorescence of lipofuscin granules.

In hippocampal sections from elderly control subjects, weak granular 14-3-3-like IR (anti-14-3-3 COM) was observed in neuronal cytoplasm and processes of some hippocampal pyramidal neurons in all cases.

In the hippocampus of PBD brains, the anti-14-3-3 COM antibody immunolabeled some neuronal cytoplasm and many Pick bodies (Fig. 1B). This immunoreactivity was abolished when the antigen peptide (14-3-3 COM) was added to the solution containing the primary antibody (Fig. 1C).

Pick bodies in hippocampal pyramidal neurons (Fig. 1D and E) and in granule cells in the dentate gyrus (Fig. 1F and G) were clearly immunolabeled by this anti-14-3-3 COM antibody.

Hyppocampal neurons were stained with the anti-sigma antibody both in control (Fig. 2A) and PBD brains (Fig. 2B and C). Although granule cells in the dentate gyrus, where

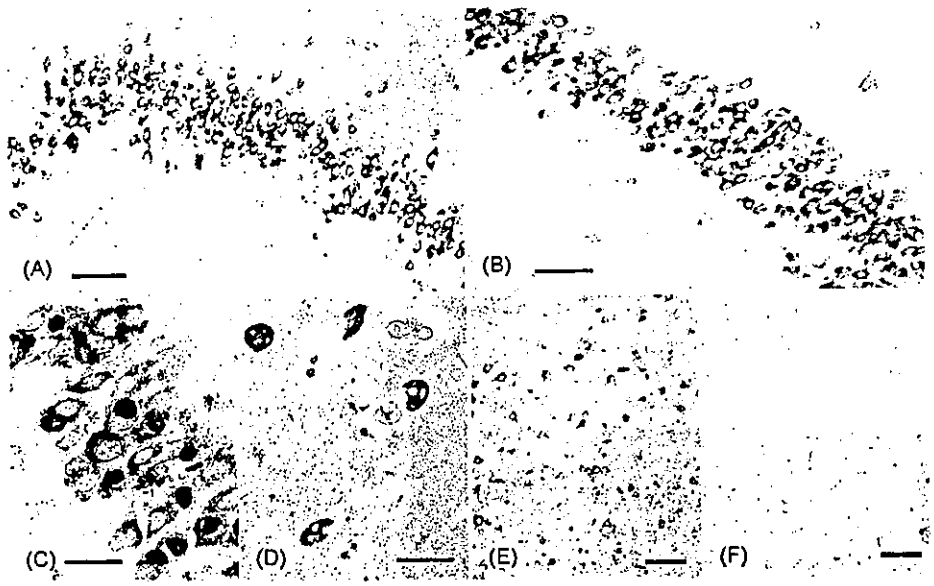

Fig. 2. (A–C) Granule cells in the dentate gyrus of control section (A) and Pick body disease brain (B and C) were immunolabeled for the sigma isoform. Numerous Pick bodies immunopositive for sigma isoform. (D) Anti-beta isoform antibody immunolabels Pick bodies, some of which contain unstained regions inside them. (E and F) Hippocampal neurons were immunolabeled for the sigma isoform (E). This immunoreactivity was abolished when the antigen peptide was added to the solution containing the primary antibody (F). Bar (A, B, E, and F) 50 μm; (C and D) 20 μm.

frequent appearance of Pick bodies is the rule, this sigma isoform-like immunoreactivity was far more intense in Pick bodies in these granule cells (Fig. 2 B and C) than those in other cortical areas. Neuropil of the cerebral cortex was homogeneously stained with the anti-epsilon antibody (data not shown). When probed with either anti-beta, anti-eta, anti-gamma, anti-tau, or anti-zeta isoform-specific antibody against 14-3-3, Pick bodies in PBD brains, as well as neurons in controls, exhibited immunostaining pattern similar to that observed with the anti-14-3-3 COM. Immunolabeling for these isoforms was less intense than that for 14-3-3 COM (data not shown). 14-3-3-like immunoreactivity in Pick bodies was not homogenous and some unstained areas were sometimes detected in Pick bodies, as shown with the anti-beta isoform-specific (Fig. 2D). Those isoform-related immunoreactivities were also abolished when each isoform antigen peptide was added to the solution containing the primary antibody (Sigma isoform-like immunoreactivity in hippocampal neurons in control brains and its effacement upon coincubation with the isoform-specific peptide, as shown in Fig. 2E and F, respectively).

Fig. 3 shows immunolocalization of 14-3-3 proteins (FITC: green) and PHF-tau (AT8-Rhodamin Red: red) in the hippocampus. The 14-3-3 epitope was colocalized to around 80% Pick bodies immunolabeled for PHF-tau.

The anti-14-3-3 antibodies used in the present study probed a single band of 30 kDa that corresponds to an expected molecular weight of 14-3-3 proteins on Western blot [16]. Immunohistochemical labeling, as well as the immunoreactive bands on Western blot [16], was abolished when the primary antibody (14-3-3 COM, zeta isoform [16] or sigma isoform) was coincubated with the corresponding antigen peptide (Fig. 1B and C for 14-3-3 COM, and Fig. 2A–D for 14-3-3 sigma).

It has been reported that 14-3-3 proteins, potentially binds to the microtubule-binding region of tau, regardless of phosphorylation state of tau [6]. In addition, it potentially stimulates phosphorylation of recombinant tau by activating protein kinase A and neuronal cdc2-like kinase. Another report [1] demonstrated that zeta isoform dimer simultaneously binds and bridges tau and GSK3β and stimulates GSK3β-catalyzed tau phosphorylation. These lines of evidence suggest that possible participation of 14-3-3 proteins in phosphorylation of tau. Indeed, presence of 14-3-3 epitope in neurofibrillary tangles in Alzheimer disease brains [12,16] is compatible with this interpretation. The present study demonstrated immunolocalization of 14-3-3 proteins in Pick bodies, another deposits with phosphorylated tau. Although we do not yet know whether the mechanism of tau phosphorylation in PBD is similar to that in AD, immunolocalization of GSK 3β in Pick bodies [4] suggest that this enzyme has potential relevance to tau phosphoryaltion both in AD and PBD. It is, then, possible that 14-3-3 proteins, potentially related to activation of GSK 3β, may also play some role during tau phosphorylation both in AD and Pick body disease. This was further confirmed by multilabeling method with PHF-tau.

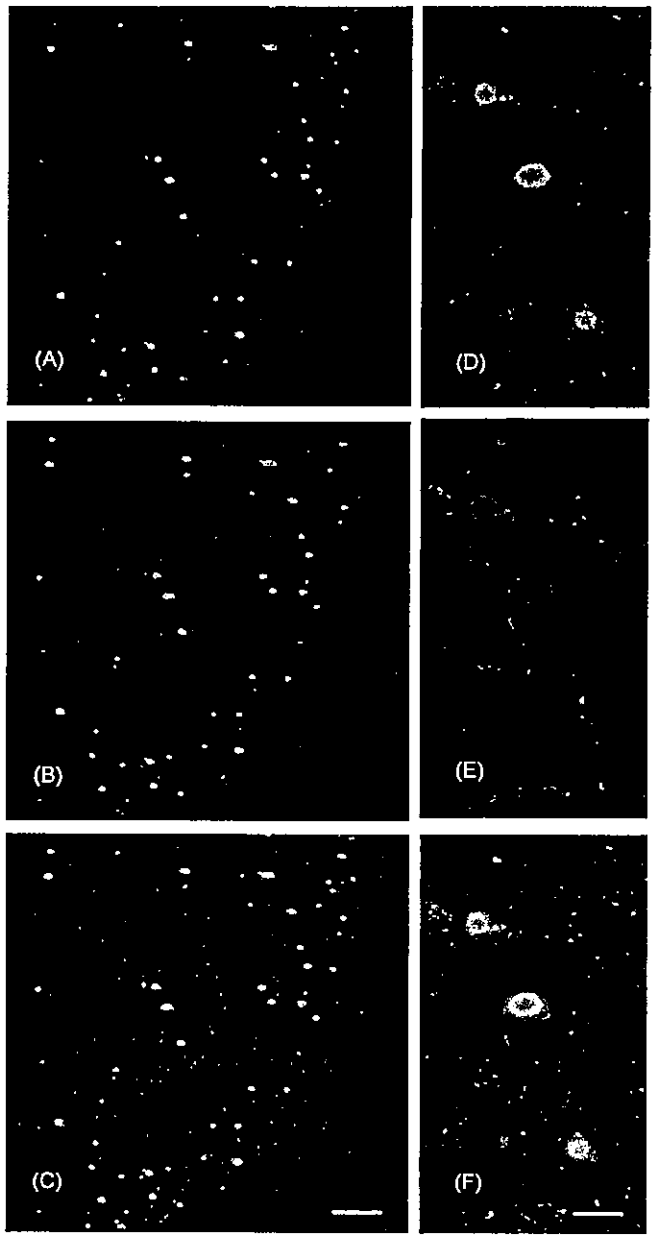

Fig. 3. Double-fluorescence labeling of Pick bodies. (A and D) Green, 14-3-3 COM visualized with FITC. (B and E) Red, phosphorylated tau (AT8) epitope visualized with Rhodamin Red. (C and F) Merged image of (A and B) and (D and E) respectively. Most of the Pick bodies, immunoreactive to AT8 (red), are also positive for 14-3-3 COM (green). Bar (C) 50 μm and (F) 20 μm.

Possible participation of 14-3-3 protein in tau phosphorylation is, however, challenged because accumulation of this protein is not restricted to tau deposits but also has been reported in a variety of deposits such as glial or neuronal cytoplasmic inclusions of multiple system atrophy [9,11] or Lewy bodies [10]. 14-3-3 proteins may, therefore, play some different roles dependent of each process. One of the possibilities, however, may include that this protein is involved in a mechanism shared by the formation of protein deposits regardless of the molecular constituents of each deposit.

Table 1
Imuunolabeling pattern of 14-3-3 isoforms in four distinct inclusions

	Pick body (Pick BD)	NFTs (AD) [16]	GCI and NCI (MSA) [9]
14-3-3 proteins	++	++	+
Sigma isoform	+ (D: ++)	+	SI
Zeta	+	++	+
Beta	+	+	+
Gamma	+	+	+
Epsilon	+	+	+
Eta	+	+	NE
Tau	+	+	NE

+: positive; ++: strongly positive; Pick BD: Pick body disease; AD: Alzheimer's disease; MSA: multiple system atrophy; D: inclusions in granule cells in dentate gyrus; GCI: glial cytoplasmic inclusions; NCI: neuronal cytoplasmic inclusions; SI: scarcely immunostained; NE: not examined.

It is interesting if different functions of 14-3-3 proteins are related to difference in their isoforms, because each isoform has different functions under different conditions [6,16,17]. We then used a panel of antibodies specific for each isoform of 14-3-3 proteins. Table 1 shows immunolabeling profile of each isoform of four distinct inclusions. Zeta isoform is preferentially accumulated in NFTs in AD brains while sigma isoform is abundant in Pick bodies in dentate granule cells. This difference suggests that 14-3-3 proteins and its isoforms are differently expressed in different pathological conditions, probably involved in different processes. It was unexpected that Pick bodies are immunopositive for the sigma isoform, because the expression of this isoform has been considered to be limited to extraneuronal cells outside the nervous system [3]. We were, however, successful in demonstrating in normal brain tissue a single band (Fig. 1A) and neuronal labeling (Fig. 2A, E and F) both immunoreactive for sigma isoform and absorbed upon coincubation with the antigen peptide. Preferential accumulation of 14-3-3 protein and its relation to isoform is summarized as Table 1. Possible accumulation of sigma isoform in pathological deposits such as Pick body is in agreement with a previous observation by Kawamoto et al. [9] that glial and neuronal cytoplasmic inclusions in multiple system atrophy are scarcely positive for sigma isoform. Further studies using isoform-specific antibodies is necessary if isoform-specificity has pathological relevance to deposit formation shared by these neurodenerative conditions (Table 1). Growing body of evidence, however, suggests that potential functions of this group of proteins are too variable to be interpreted, at least at present, on unified hypothesis to explain these degenerative processes.

Molecular, as well as topographical, dissection of 14-3-3 proteins and its isoforms in relation to normal and pathological functions and structures will provide us with improved understanding of this molecule.

Acknowledgments

This work is supported in part by grants for Sumitimo Welfare Foundation. We are grateful to Dr. Kazuko Aoki-Yoshino for her help for Western blotting.

References

[1] A. Agarwal-Mawal, H.Y. Qureshi, P.W. Cafferty, Z. Yuan, D. Han, R. Lin, H.K. Paudel, 14-3-3 connects glycogen synthase kinase-3β to tau within a brain microtubule-associated tau phosphorylation complex, J. Biol. Chem. 278 (2003) 12722–12728.

[2] K. Aoki, T. Uchihara, N. Sanjo, A. Nakamura, K. Ikeda, K. Tsuchiya, Y. Wakayama, Increased expression of neuronal apolipoprptein E in human brain with cerebral infarction, Stroke 34 (2003) 875–880.

[3] D. Berg, C. Holzmann, O. Riess, 14-3-3 proteins in the nervous system, Nat. Rev. Neurosci. 4 (2003) 752–762.

[4] I. Ferrer, M. Barrachina, B. Puig, Glycogen synthase kinese-3 is associated with neuronal and glial hyperphosphorylated tau deposits in Alzheimer's disease, Pick's disease, progressive supranuclear palsy and coticobasal degeneration, Acta Neuropathol. 104 (2002) 583–591.

[5] H. Fu, R.R. Subramanian, S.C. Masters, 14-3-3 proteins: structure, function, and regulation, Annu. Rev. Pharmacol. Toxicol. 40 (2000) 617–647.

[6] M. Hashiguchi, K. Sobue, H.P. Paude, 14-3-3 ζ is an effector of tau protein phosphorylation, J. Biol. Chem. 275 (2000) 25247–25254.

[7] G. Hsich, K. Kenney, C.J. Gibbs, K.H. Lee, M.G. Harrington, The 14-3-3 protain in cerebrospinal fluid as a maker for transmissible spongiform encephalopathy, N. Engl. J. Med. 335 (1996) 924–930.

[8] T. Ichihara, T. Isobe, T. Okuyama, T. Yamauchi, H. Fujisawa, Brain 14-3-3 protein is an activator protein that activates tryptophan 5-monooxygenase and tyrosin 3-monooxygenase in the presence of Ca^{2+}, calmodulin-dependent protein kinase II, FEBS Lett. 219 (1987) 79–82.

[9] Y. Kawamoto, I. Akiguchi, S. Nakamura, H. Budka, Accumulation of 14-3-3 proteins in glial cytoplasmic inclusions in multiple system atrophy, Ann. Neueol. 52 (2002) 722–731.

[10] Y. Kawamoto, I. Akiguchi, S. Nakamura, Y. Honjyo, H. Shibasaki, H. Budka, 14-3-3 proteins in Lewy bodies in Parkinson disease and diffuse Lewy body disease brain, J. Neuropathol. Exp. Neurol. 61 (2002) 245–253.

[11] T. Komori, K. Ishizawa, N. Arai, T. Hirose, T. Mizutani, M. Oda, Immunoexpression of 14-3-3 proteins in glial cytoplasmic inclusions of multiple system atrophy, Acta Neuropathol. 103 (2003) 66–70.

[12] R. Layfield, J. Fergusson, A. Aitken, J. Lowe, L. Landon, Neurofibrillary tangles of Alzheimer's disease brain contain 14-3-3 protein, Neurosci. Lett. 209 (1996) 57–60.

[13] M. Rosenquist, 14-3-3 proteins in apoptosis, Braz. J. Med. Biol. Res. 36 (2003) 403–408.

[14] K. Tsuchiya, M. Ikeda, K. Hasegawa, T. Fukui, T. Kuroiwa, C. Haga, S. Oyanagi, I. Nakano, M. Matsushita, S. Yagishita, K. Ikeda, Distribution of cerebral cortical lesions in Pick's disease with Pick bodies: clinicopathological study of six autopsy cases showing unusual clinical presentation, Acta Neuropathol. 102 (2001) 553–571.

[15] T. Uchihara, K. Ikeda, K. Tsuchiya, Pick body disease and Pick syndrome, Neuropathology 23 (2003) 318–326.

[16] T. Umahara, T. Uchihara, K. Tsuchiya, A. Nakamura, T. Iwamoto, K. Ikeda, M. Takasaki, 14-3-3 proteins and zeta isoform containing neurofibrillary tangles in patients with Alzhrimer's disease, Acta Neuropathol. (published online July 2004).

[17] H. Wakabayashi, M. Yano, N. Tachikawa, S. Oka, M. Maeda, H. Kido, Increased concentration of 14-3-3 epsilon, gamma, and zeta isoforms in cerebrospinal fluid of AIDS patients with neuronal destruction, Clin. Chim. Acta 312 (2001) 97–105.

[18] J. Zha, H. Harada, E. Yang, J. Jockel, S.J. Korsmeyer, Serine phosphorylation of death agonist BAD in response to survival factor results in binding to 14-3-3 not BCL-X(L), Cell 87 (1996) 619–692.

RESEARCH ARTICLE

Profound Cardiac Sympathetic Denervation Occurs in Parkinson Disease

Takeshi Amino[1,2,5]; Satoshi Orimo[1,2]; Yoshinori Itoh[3]; Atsushi Takahashi[4]; Toshiki Uchihara[2]; Hidehiro Mizusawa[5]

[1] Department of Neurology, Kanto Central Hospital, Tokyo, Japan.
[2] Department of Neuropathology, Tokyo Metropolitan Institute for Neuroscience, Japan.
[3] Department of Internal Medicine, [4]Department of Organ and Function Pathology, Yokufukai Geriatric Hospital, Tokyo, Japan.
[5] Department of Neurology and Neurological Science, Tokyo Medical and Dental University, Japan.

Corresponding author:
Satoshi Orimo, MD., Department of Neurology, Kanto Central Hospital, 6-25-1 Kami-Yoga, Setagaya-ku, 158-8531, Tokyo, Japan (E-mail: orimo@kanto-ctr-hsp.com)

In the last few years, cardiac sympathetic dysfunction in Parkinson disease (PD) has been postulated on the basis of decreased cardiac uptake of sympathoneural imaging tracers. However, the pathological substrate for the dysfunction remains to be established. We examined the left ventricular anterior wall from postmortem specimens with immunohistochemical staining for tyrosine hydroxylase (TH), neurofilament (NF) and S-100 protein in PD patients and control subjects, and quantified the immunoreactive areas. As TH-immunoreactive axons nearly disappeared and NF-immunoreactive axons drastically decreased in number, the morphological degeneration of the cardiac sympathetic nerves in PD was confirmed. Quantitative analysis showed that sympathetic nerves were preferentially involved. Triple immunofluorolabeling for NF, TH, and myelin basic protein showed clearly the profound involvement of sympathetic axons in PD. The extent of involvement of the cardiac sympathetic nerves seems likely to be equivalent to that in the central nervous system, including the nigrostriatal dopaminergic system. PD affects the cardiac sympathetic nervous system profoundly as well as nigrostriatal dopaminergic system.

Brain Pathol 2005;15:29-34.

INTRODUCTION

Parkinson disease (PD) is not only a disease of the nigrostriatal dopaminergic system but also a disease of the autonomic nervous system. Therefore, symptoms of autonomic dysfunction such as constipation, orthostatic and postprandial hypotension, dyshidrosis and bladder dysfunction occur commonly in PD (32).

Recent awareness of a decrease in cardiac uptake of [^{123}I]*meta*-iodobenzylguanidine (MIBG) on single photon emission computed tomography (SPECT) or of 6-[^{18}F]fluorodopamine (6F-DA) on positron emission tomography (PET) in PD patients is now attracting increasing attention because this decreased uptake is detectable before other autonomic disturbances are evident (6, 24, 39). Moreover, this decrease is of particular clinical importance because it is usually undetectable in patients with multiple system atrophy (MSA), progressive supranuclear palsy (PSP) (39) or corticobasal degeneration (CBD) (23) and could therefore be helpful in isolating PD from among the various parkinsonian syndromes.

The decreased cardiac uptake of these sympathoneural radiotracers may represent dysfunction of the cardiac sympathetic system in PD (6). Indeed, our recent immunohistochemical study demonstrated a marked decrease in tyrosine hydroxylase (TH)-immunoreactive+ axons in the epicardium of the left ventricular anterior wall in PD patients (22, 25). This pathological finding was considered to represent the involvement of the cardiac sympathetic nerves in PD and presumably accounts for the decreased cardiac uptake of the tracers. However, it remains to be clarified whether morphological depletion of the sympathetic nerves and denervation occurs or whether they are merely functionally involved, and whether TH+ axons are selectively affected.

In this case-control study, we observed neurofilament (NF)-immunoreactive axons coupled with TH+ axons, and quantified the frequency of TH+ axons relative to NF+ axons. In addition, we investigated their relation to myelin and Schwann cells. Triple immunofluorolabeling for NF, TH and myelin basic protein (MBP) demonstrated clearly the profound involvement of TH+ axons in PD patients.

MATERIALS AND METHODS

Subjects. Cardiac tissue samples obtained at autopsy from four PD patients and 5 control subjects were used in this study. Clinical diagnosis of PD was based on dopa-responsive parkinsonian symptoms (tremor, muscle rigidity, akinesia and postural instability). The postmortem examination revealed marked neuronal loss and numerous Lewy bodies in the substantia nigra, locus ceruleus and dorsal vagal nucleus. Five control subjects without parkinsonian symptoms and signs, primary heart disease, diabetes mellitus and peripheral neuropathy, were enrolled. The postmortem examinations confirmed the absence of Lewy bodies in the central nervous system. There was no statistical difference in age between the PD patients and control subjects. (Table 1)

Immunohistochemical staining. The heart tissue was fixed in formalin at autopsy within 48 hours after death. Specimens were obtained from the left ventricular anterior wall and embedded in paraffin. The left ventricular wall was considered preferable for this study because PET or SPECT studies in healthy subjects show uniformly high radioactivity there. Four-micrometer thick sections sliced axially were deparaffinized and stained with hematoxylin and eosin (H&E).

We used the following primary antibodies for immunohistochemical staining: anti-NF (SMI-31, mouse monoclonal, 1:10000 SMI, Baltimore, Md) as a marker

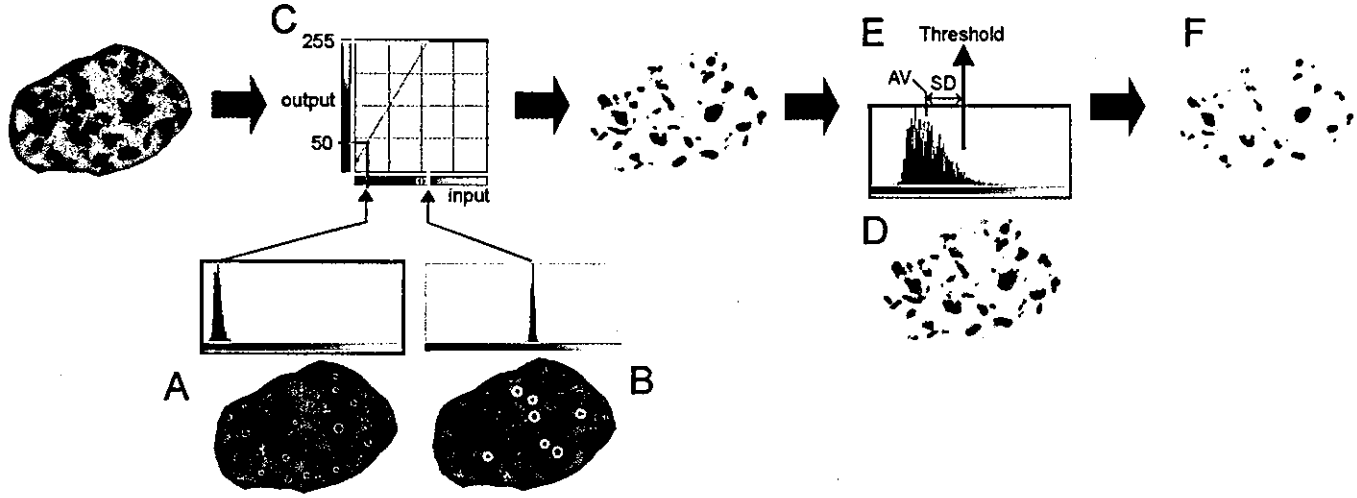

Figure 1. *Procedure for measuring immunoreactive areas.* **A.** On an 8-bit gray scale (0:black-255:white) image, several areas with the most intense immunoreactivity were circled and the mean value of these areas was calibrated to 50 on the 8-bit gray scale. **B.** In the same way, the mean value of several unstained areas was calibrated to 255. **C.** Based on these 2 calibration points, the entire image was transformed linearly into an 8-bit gray scale. **D.** On the transformed image, immunostained axonal areas were arbitrarily selected and their average value (AV) and standard deviation value (SD) were calculated. **E.** The entire image was then binarized with the threshold defined as the AV ± SD. **F.** Areas with a pixel value below the threshold were judged immunoreactive areas. Extracted areas were therefore considered reasonable as immunoreactive areas compared with the original digitalized image.

Case	Age at death	Gender	Duration of disease (years)	Hoehn and Yahr stage	Cause of death
PD 1	70	Male	10	5	Bronchitis
PD 2	82	Female	10	4	Colon cancer, ileus, sepsis
PD 3	83	Female	>3	5	Pneumonia
PD 4	91	Female	15	4	Pneumonia, chronic lymphocytic leukemia
Control 1	86	Female	-	-	Colon cancer
Control 2	89	Male	-	-	Esophageal cancer, pneumonia
Control 3	81	Female	-	-	Colon cancer, peritonitis
Control 4	93	Male	-	-	Acute respiratory failure, tracheitis
Control 5	91	Female	-	-	Acute respiratory failure, emphysema

Table 1. Characteristics of patients and control subjects.

for all axons, anti-TH (mouse monoclonal, 1:3000 SIGMA, Saint Louis, Mo) as a marker for catecholaminergic axons, anti-S-100 protein (mouse monoclonal, 1:1500 IBL, Gunma, Japan) as a marker for Schwann cells and anti-MBP (rabbit polyclonal, 1:1000 IBL) as a marker for myelin. An indirect immunofluorescence procedure using the avidin-biotin technique was employed. The deparaffinized sections were treated in a microwave oven with citrate buffer 3 times for 6 minutes, treated with 1% hydrogen peroxide for 30 minutes and then incubated with the primary antibody diluted with phosphate-buffered saline containing 0.03% Triton-X100 and the corresponding blocking serum. In order to reduce background stain and achieve optimal signal to noise ratio, we usually take 2 days or longer at 4°C for primary antibody incubation with higher dilution. The sections were then incubated for 2 hours with the biotinylated secondary antibody (anti-rabbit or anti-mouse, 1:1000, Vector, Burlingame, Calif), followed by avidin-biotin-peroxidase complex (1:1000 ABC Elite, Vector). The peroxidase labeling was visualized with diaminobenzidine-nickel as chromogen, and then the stained sections were lightly stained with fast nuclear red solution.

Quantification procedure. Relatively large (diameter >50 μm) and round (maximum diameter/minimum diameter <2) nerve fascicles in the epicardium were all selected to quantify the immunoreactive areas. This elimination of oval fascicles (maximum diameter/minimum diameter ≥2) allowed us to avoid quantifying tangentially oriented axons. The selected fascicles were captured by a digital camera (D1, Nikon, Tokyo, Japan) connected to a microscope (BX-50, Olympus, Tokyo, Japan) with an objective ×40. The contour of the endoneurium was traced on a digitizer coupled with a liquid crystal display (PL-400, Wacom, Saitama, Japan). On the digitalized 8-bit RGB image of each endoneurium, the area of the entire endoneurium (fascicle area), TH+ area and NF+ area were measured using a standardized procedure on software (Adobe Photoshop 5.5 and NIH-image 1.62) as shown in Figure 1. Firstly, each digitalized image was transformed into an 8-bit gray scale (0:black-255:white) as follows. Several areas with the most intense immunoreactivity were selected and the mean value of these areas was calibrated to 50 on the 8-bit gray scale. In the same way, the mean value of several unstained areas was calibrated to 255. Based on these 2 calibration points, the entire image was transformed linearly into an 8-bit gray scale. This procedure enabled us to minimize the difference of brightness among the original digitalized images. Based on this transformed image, the average value (AV) and standard deviation value (SD) of stained axonal areas, which were arbitrarily selected, were calculated. The entire image was then binarized with the threshold defined as AV+SD. Areas with a pixel value below the threshold were judged to be immunoreactive areas. Finally the extracted areas were considered reasonable as immunoreactive areas compared with the original digitalized image.

Quantified values from several nerve fascicles from each subject were summed to yield the total fascicle area, total TH+ area and total NF+ area. The ratios of the total TH or NF+ area to the total fascicle area (TH/fascicle of NF/fascicle), the ratio of the total TH+ area to the total NF+ area (TH/NF) and the difference between the total TH+ areas and the total NF+ areas (NF-TH) were calculated for each subject. Differences in these calculated values between the PD and control groups were analyzed with the Mann-Whitney U test.

Triple immunofluorolabeling. Deparaffinized sections from a patient and a control subject were treated in a microwave oven with citrate buffer 3 times for 6 minutes, and then with 2% hydrogen peroxide for 30 minutes. Firstly, they were incubated with the anti-MBP antibody (diluted to 1:9000, which is detectable after catalyzed reporter deposition amplification) at 4°C for 2 days. They were incubated with anti-rabbit IgG made from goat conjugated to horseradish peroxidase (HRP, 1:1000; Pierce, Rockford, Ill). The HRP signal was amplified with biotinylated tyramide (1:1000; Perkin-Elmer, Boston, Mass) and then visualized with Cy-5 conjugated to streptavidin (1:200; Kirkegaard & Perry, Gaithersberg, Md). Subsequently, sections were incubated with a mixture of the anti-NF mouse monoclonal antibody (1:1000) and the anti-TH rabbit polyclonal antibody (1:100) at 4°C for another 2 days in the dark. These 2 antibodies were visualized with a mixture of anti-mouse IgG made from sheep conjugated with rhodamine (1:200, Jackson ImmunoResearch, West Grove, Pa) and anti-rabbit IgG made from goat conjugated with FITC (1:200, Vector), which could selectively visualize the anti-TH antibody because of insufficient sensitivity to the diluted anti-MBP antibody (20, 34).

RESULTS

H&E and immunohistochemical staining (Figure 2). H&E staining of the sections revealed several nerve fascicles, mostly transverse-sectional, in the epicardium. There was no apparent difference in the number and size of those nerve fascicles between the control and PD groups.

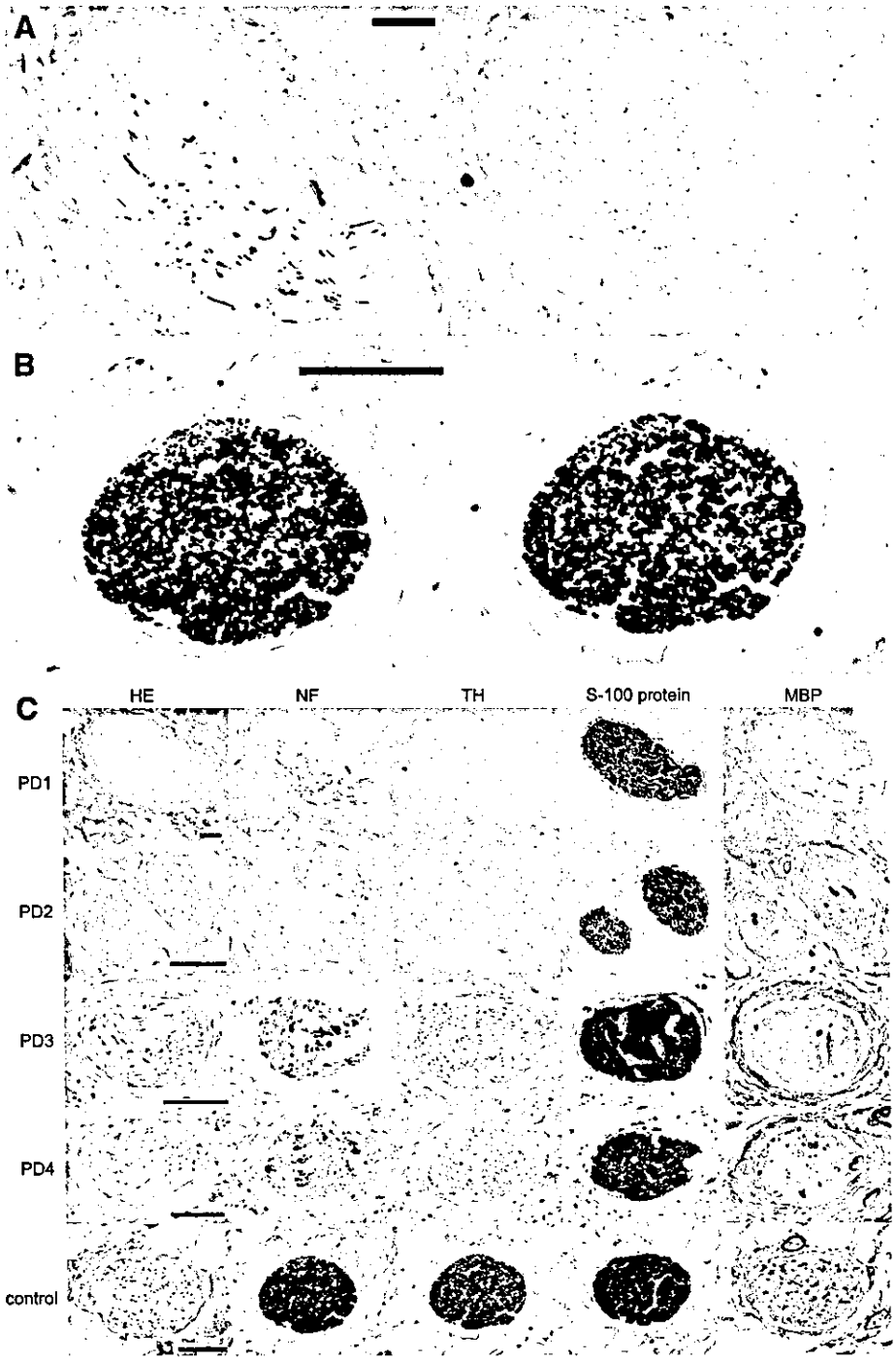

Figure 2. *H&E and immunohistochemical staining.* **A.** In the PD patient (PD 1), neurofilament (NF)-immunoreactive axons (Left) were sparse and tyrosine hydroxylase (TH)-immunoreactive axons (Right) were nearly absent. **B.** The control subject (control 4) showed numerous NF-immunoreactive axons (Left) and TH-immunoreactive axons (Right). **C.** Representative nerve fascicle in each patient or control subject (control 4) were shown. In all patients, NF-immunoreactive axons and TH-immunoreactive axons drastically decreased in number whereas S-100 protein-immunoreactive structures were equally preserved. A few myelin basic protein (MBP)-immunoreactive structures were seen in the fascicles of the epicardium and the number was smaller in patients than in control subjects. Scale bar = 100 μm.

In the control subjects, numerous NF+ axons were shown in the fascicle. Many TH+ axons were also seen, although they were smaller in number than NF+ axons. S-100 protein+ structures were also numerous, whereas MBP+ structures were comparatively sparse.

In the PD patients, NF+ axons were sparse and TH+ axons were nearly absent. A few MBP+ structures were seen, but the

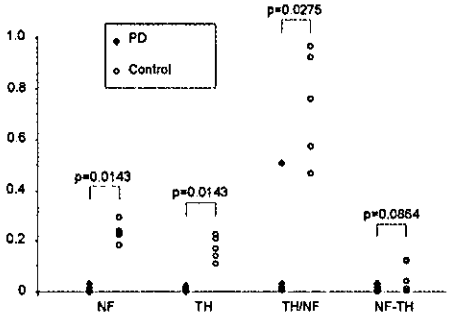

Figure 3. *Results of quantification for immunoreactive areas.* Mann-Whitney U tests were used for the statistical analysis between the patient (PD) and control group(Control).

number was smaller than in the control subjects. S-100 protein+ structures were numerous and equally preserved compared with those in the control subjects.

Quantitative analysis (Figure 3). In the control subjects, the ratios of TH/NF, which were in the range of 47% to 97%, revealed that most of the axons in the nerve fascicles in the epicardium were immunoreactive to TH. Both ratios of TH/fascicle and NF/fascicle obviously and significantly decreased in the PD group. The ratio of TH/NF also significantly decreased in the PD group. On the other hand, the difference of NF-TH showed a tendency to be smaller in the PD group, although it did not reach statistical significance.

Triple immunofluorolabeling (Figure 4). In the control subject (Figure 4B), numerous NF+ axons (red) were observed in nerve fascicles and most were immunoreactive to TH (green). MBP+ structures (blue) were sparse, and some surrounded TH+ axons as well as TH- axons. In the PD patient (Figure 4A), a fairly small number of NF+ axons and fewer MBP+ structures were recognized but TH+ axons were absent.

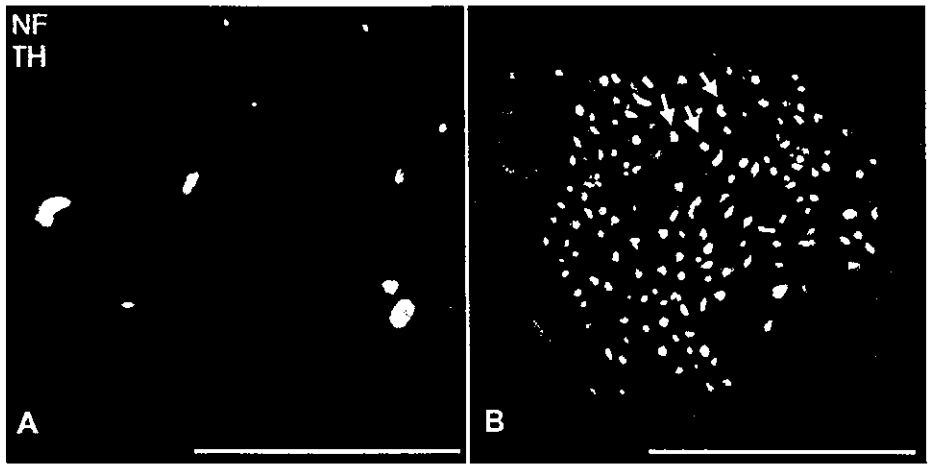

Figure 4. *The nerve fascicles in the epicardial spaces immunofluorolabeled with anti-NF (red), anti-TH (green) and anti-MBP (blue) antibodies.* **A.** PD patient. **B.** Control subject. In PD (**A**), TH-immunoreactive nerve fibers almost disappeared, and NF-immunoreactive nerve fibers and MBP-immunoreactive structure were markedly decreased. In the control subject (**B**), most NF-immunoreactive nerve fibers were also immunoreactive to TH (yellow), and, some were surrounded by MBP-immunoreactive structures (arrow in B). Scale bar = 50 μm.

DISCUSSION

In the last few years, cardiac sympathetic dysfunction in PD has been revealed by the decreased cardiac uptake of sympathoneural tracers detected in SPECT or PET studies. We recently reported a marked decrease in TH+ axons in PD patients based on histological examination of the epicardium of the left ventricular anterior wall. Furthermore, in this case-control study, we expanded this observation by quantifying TH+ axons and NF+ axons in a series of patients with or without PD.

Immunohistochemical staining revealed that the nerve fascicle in the epicardium contains a large number of TH+ axons in normal individuals. The high proportion of TH/NF in quantitative analysis indicated that TH+ axons occupy more than half of all axons in each fascicle. This TH+ dominant proportion is consistent with the previously reported ratio of catecholaminergic axons to cholinergic axons in the ventricular myocardium (2, 11). TH is a rate-limiting enzyme in catecholamine synthesis. The presence of TH in an axon is considered to indicate that the axon is catecholaminergic, and it has been used as a marker for locating presumptive sympathetic neural tissue (18). Recent studies demonstrated that TH could be also present in non-sympathetic tissue, such as the cranial parasympathetic ganglia of rat (9) or human cardiac ganglia (31), while its functional relevance in relation to the nature of the axons remains speculative. The existence of TH, therefore, is unable to prove conclusively by itself that the tissue is sympathetic. However, in the myocardium, noradrenalin is the dominant species among catecholamines (21, 28) and its tissue concentration is drastically reduced after stellectomy in rats (14, 27) and guinea pigs (7). This suggests that TH+ axons in the epicardium of the left ventricle presumably represent sympathetic axons, mainly noradrenergic axons originating from the cervico/thoracic sympathetic ganglia. The disappearance of TH+ axons in transplanted human hearts (30, 37) also indicates that TH+ axons are extrinsic, and is compatible with this interpretation.

The immunohistochemical staining for NF and TH showed a drastic decrease of NF+ axons and a more profound decrease of TH+ axons in PD. This finding indicated not merely the loss of the catecholamine synthesis enzyme, TH, but also the depletion of the sympathetic axons themselves. It means that the cardiac sympathetic nerves are morphologically degenerated. This offered new morphological evidence for the involvement of the cardiac sympathetic nerves in addition to the functional evidence that had been shown by PET or SPECT studies.

The near complete disappearance of TH+ axons and significant decrease in TH/NF in the PD group show that the sympathetic nerves were profoundly and preferentially involved in PD patients. On the other hand, NF-TH, that represents TH- axons, tended to be less frequent in PD, although the difference was not statistically significant. It is therefore possible that TH- axons are not involved. The PD related-depletion of TH- axons, if present, could have been overlooked because of the small number of TH- axons, leaving the possibility that the non-catecholaminergic axon is also involved in PD. Although the origin and nature of these non-catecholaminergic axons remain speculative, they may be from intrinsic neurons where Lewy bodies were previously found (10, 36).

According to PET or SPECT study, the extent of involvement in PD seems to vary